

A Universal Space-Time Architecture for Multiple-Antenna Aided Systems

Shinya Sugiura, *Member, IEEE*, Sheng Chen, *Fellow, IEEE*, and Lajos Hanzo, *Fellow, IEEE*

Abstract—In this tutorial, we first review the family of conventional multiple-antenna techniques, and then we provide a general overview of the recent concept of the powerful Multiple-Input Multiple-Output (MIMO) family based on a universal Space-Time Shift Keying (STSK) philosophy. When appropriately configured, the proposed STSK scheme has the potential of outperforming conventional MIMO arrangements.

Index Terms—MIMO, space-time coding, space-time shift keying, wireless communication.

I. INTRODUCTION

AGAINST the recent background of rapidly-increasing demand for high-speed multimedia wireless transceivers communicating over dispersive fading channels, a bandwidth efficient and reliable transmission technology is desired. Multiple-Input Multiple-Output (MIMO) techniques constitute promising solutions, where multiple Antenna Elements (AEs) are employed at a transmitter and/or a receiver in conjunction with appropriate space-time coding and modulation. The exploitation of the spatial dimension provides a wireless system with an additional degree of freedom, hence facilitating the attainment of additional diversity gains, multiplexing gains and beamforming gains. As a result of two decades of intensive investigations, the field of MIMO theory and practice has substantially matured.

More explicitly, the pioneering studies by Foschini [1], [2] and by Telatar [3] revealed that MIMO systems have the potential of attaining a higher rate upon increasing the number of AEs, which is achieved without requiring additional bandwidth and transmission power. More explicitly, there is a linear relationship between the channel capacity and the number of AEs employed. By contrast, several years prior to the invention of this high-rate MIMO architecture aiming for spatial multiplexing, the philosophy of Space-Time Codes (STCs), including Space-Time Block Codes (STBCs) [4], [5] and Space-Time Trellis Codes (STTCs) [6], was proposed, which constitutes another core class of MIMO systems. This transmit diversity concept is capable of combating the detrimental effects of fading channels, by exploiting the maximum achievable diversity order. Importantly, regardless of the

type of MIMO gains, we exploit both the space- and time-dimensions for space-time processing.

Considering the powerful capability of MIMO techniques, it is a natural direction to include them in wireless architectures. In particular, depending on the desirable MIMO gain, MIMO techniques may be classified into four different categories, such as diversity, multiplexing, multiple access and beamforming techniques, as shown in Fig. 1. In order to provide further insights, these four MIMO types are briefly summarized below.

A. Spatial Diversity

Spatial diversity [7] techniques rely on multiple AEs in order to improve the attainable system performance in fading channels. More specifically, spatial diversity is based on the concept of efficiently combining the received signals associated with the different pairs of transmit and receive AEs, which experience independent fading paths imposed by the random fluctuations of the received signal levels. The AEs have to be spaced sufficiently far apart for the sake of attaining a diversity gain from the gleaned independently-faded received signal replicas. Since the minimum antenna separation required for fading is approximately 0.38λ [8], the desirable antenna separation experiencing sufficiently independent fading is on the order of ten times the wavelengths. A further attractive feature of spatial diversity is that it does not sacrifice additional time slots, neither does it reduce the spectrum efficiency in comparison to classic time- and frequency-diversity schemes. To be specific, the maximum attainable diversity order is equal to $(M \cdot N)$, where M and N are the number of transmit and receive AEs, assuming that the channel between each transmit-receive antenna pair is faded independently.¹

Furthermore, spatial diversity techniques may be divided into two classes, namely receive diversity and transmit diversity. Receive diversity is the classic technique, where the independently fading multiple paths are combined at the receiver side. The Base Station (BS) has significant space to allow the installation of multiple AEs spaced sufficiently far apart, in order to achieve receive diversity in uplink scenarios. More specifically, the diverse techniques of coherent signal combining were developed depending on the specific treatment

Manuscript received 3 August 2010; revised 18 January 2011. The financial support of the EPSRC, UK under the auspices of the India-UK Advanced Technology Centre (IU-ATC) and that of the RC-UK under the China-UK Science bridge in Wireless Communications is gratefully acknowledged.

S. Sugiura is with the Toyota Central R&D Laboratories, Inc., Nagakute, Aichi, 480-1192, Japan (e-mail: sugiura@ieee.org).

S. Chen and L. Hanzo are with the School of Electronics and Computer Science, University of Southampton, Southampton, SO17 1BJ, UK (e-mail: {sqc,lh}@ecs.soton.ac.uk).

Digital Object Identifier 10.1109/SURV.2011.041911.00105

¹To be more specific, this does not mean that all the STBCs achieve a unity-rate. For a high number of transmit AEs, i.e. for $M > 2$, the throughput of the orthogonal STBC scheme is reduced to less than unity, while maintaining the maximum achievable transmit diversity order of M , as shown in [9]. Furthermore, the maximum achievable diversity order varies, depending on the space-time code's structure employed, but it is upper-bounded by $(M \cdot N)$. The following sections will also detail the maximum achievable diversity order of different MIMO arrangements in a unified manner.

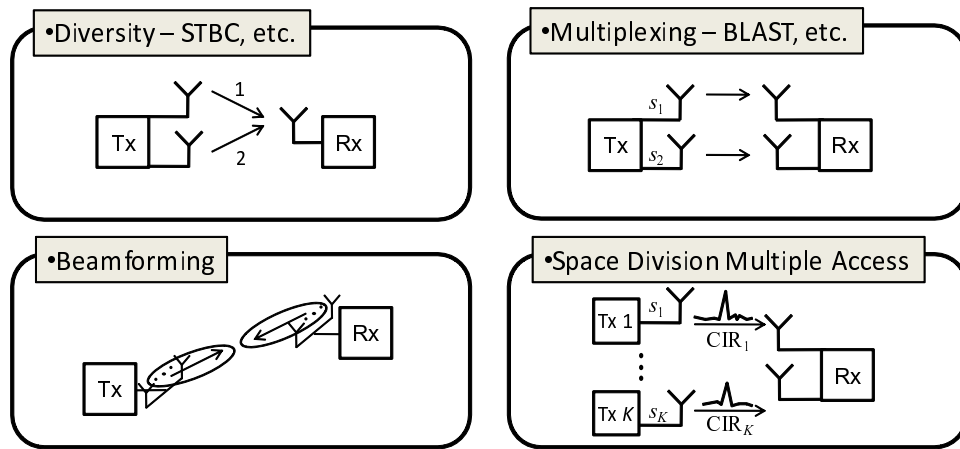


Fig. 1. Classification of four MIMO functions.

of the combined signals' phase and amplitude, which are Selection Combining (SC), threshold combining, Equal-Gain Combining (EGC) and Maximum-Ratio Combining (MRC), as summarized in [10]. Furthermore, the theoretical capacity bound of received signal combining employed in conjunction with adaptive transmission was derived in [11]. Although receive diversity is capable of achieving the maximum attainable diversity order, which is proportional to the number of receive AEs, it is often impractical to employ multiple antennas at the mobile handset's receiver.

By contrast, transmit diversity relies on multiple AEs at the transmitter, where the precoded signals are appropriately allocated to the transmit AEs and to the time slots in advance of the transmission. Hence, the employment of transmit diversity is desirable for downlink scenarios, where more antenna-installation space and processing capability are affordable at the BS. Historically, the first transmit diversity scheme was based on delay-diversity considered in the context of employing simulcasting at the BS [12] for a single-BS aided downlink [13]. In 1998 Alamouti [4] proposed a sophisticated transmit diversity scheme designed for the scenario of two transmit antennas, which enables a simple transmit diversity implementation and single-symbol-based low-complexity Maximum Likelihood (ML) detection at the receiver, while dispensing with the necessity of channel knowledge at the transmitter, but requires pilot-based Down-Link (DL) channel estimation. Since then, Alamouti's scheme has been followed by the development of diverse STBCs, such as those portrayed in [14]–[17]. By contrast, STTCs [18] were developed as the extension of conventional trellis codes [19] embedded into multi-antenna systems, which may be designed for the sake of achieving both spatial diversity as well as a space-time coding gain. Furthermore, motivated by the concept of STCs, Space-Time Spreading (STS) [20] was proposed, in order to achieve a transmit diversity gain with the aid of spreading the transmitted signals across multiple antennas in the context of Direct-Sequence Code Division Multiple Access (DS-CDMA) systems, while supporting multiple users. Another transmit diversity scheme is Cyclic Delay Diversity (CDD) [21], which was developed for generating multipath replicas in MIMO-aided Orthogonal Frequency-Division Multiplexing

(OFDM) based systems. In this scheme, the same information is transmitted from separate antenna elements, while imposing antenna-specific cyclic delays [22], hence providing a transmit diversity gain in a simple manner. Its explicit benefit is that the associated receiver structure remains essentially unchanged.

Although the above-mentioned spatial diversity schemes [4], [14]–[20] assumed that perfect Channel State Information (CSI) was available at the receiver, it is often quite challenging to acquire accurate CSI amongst all the MIMO channel elements, especially for rapidly moving vehicles, since doubling the vehicular speed requires doubling the pilot density [19]. The resultant CSI estimation errors may cause a severe degradation of the achievable performance. Since each of the MIMO subchannels has to be sampled at multiples of the Doppler frequency, at high speeds an increased pilot overhead has to be tolerated for the sake of accurately estimating each MIMO channel component, which also gives rise to a substantial increase of the CSI-estimation complexity. To this end, the class of Differential STCs (DSTCs) [23]–[28] has been proposed and developed, allowing us to dispense with any CSI estimation and hence to avoid the performance deterioration associated with imperfect CSI estimation. In [23], Tarokh *et al.* introduced a differentially-encoded counterpart of Alamouti scheme, assuming the employment of Phase Shift Keying (PSK). Additionally, the DSTCs based on Unitary Space-Time Modulation (USTM) and on group codes were proposed in [24] and [25], respectively. Furthermore, Multiple-Symbol Differential Detection (MSDD) was also developed for the sake of combating time-selective fading [26], even when the Doppler-frequency was high [27].

B. Spatial Multiplexing

In contrast to the above-mentioned spatial diversity technique, which employs multiple transmit and/or receive antennas for achieving a high diversity gain, Spatial Division Multiplexing (SDM), which is represented for example by the family of Bell Labs Layered Space-Time (BLAST) schemes [1], [29], exploits the MIMO channels for the sake of increasing the attainable transmission rate. This performance gain is referred to as multiplexing gain. More specifically, M independent signal substreams are transmitted from different

transmit AEs at the same frequency and within the same time slot, therefore the corresponding transmission rate is multiplied by the number of transmit antennas, assuming the employment of the same modulation scheme for each of the substreams.

By contrast, the SDM receiver differentiates each of the M co-channel substreams based on the knowledge of the $(M \times N)$ -element MIMO channels. Since the M substreams are multiplexed and hence interfere with each other, we have to separate the substreams with the aid of an appropriate MIMO detection algorithm [30]. The optimal ML detector has to consider all the legitimate sequences, hence its decoding complexity increases exponentially upon increasing the number of transmit AEs. To this end, an efficient ordered successive detection scheme was designed for V-BLAST in [31], and since then diverse SDM detection algorithms have been developed [32], [33]. Alternatively, the co-channel interferences associated with the MIMO channels may be reduced by employing pre-processing at the transmitter side, which requires the knowledge of the channel to be encountered. This technique is referred to as transmitter pre-processing or Multi-User Transmission (MUT) [34]. This makes the receiver's operation less complex and hence is imminently suitable for downlink scenarios. However, the potential CSI errors encountered at the transmitter may result in a substantial performance deterioration, suggesting that both an accurate DL CSI-estimates and a robust feedback channel is required for MUT.

In 1998, Foschini [35] formulated the theoretical capacity analysis of MIMO channels as the evolution of Shannon's capacity [36] presented in 1948. This study showed that the idealized MIMO capacity increases linearly upon increasing the number of transmit AEs. This capacity limit is referred to as the Continuous-input Continuous-output Memoryless Channel (CCMC) capacity, since it is defined under the assumption of continuous-amplitude discrete-time Gaussian-distributed transmitted signals, where only the transmit power and the bandwidth are restricted. The discovery of this MIMO capacity introduced a new extended limit and demonstrated the MIMO's potential of achieving a high transmission rate as well as high power and bandwidth efficiency. Moreover, in [37] the Discrete-input Continuous-output Memoryless Channel (DCMC) capacity was defined for MIMO channels in combination with the specific multi-dimensional signaling set employed.

C. Space Division Multiple Access

Space Division Multiple Access (SDMA) [38], also known as Multi-User MIMO (MU-MIMO) [39], utilizes user-specific Channel Impulse Responses (CIRs) for differentiating the supported users in uplink scenarios, and hence the achievable performance of SDMA is not affected by the supported users' locations. In SDMA system the users communicate with a BS by using the same bandwidth and time slots. Accordingly, it can be argued that SDMA is a close relative of SDM in a sense that both schemes exhibit a capacity gain by decomposing multiplexed MIMO channels into parallel channels. More specifically, SDMA utilizes this multiplexing gain in

order to increase the number of supported users, while SDM exploits it for the sake of increasing the throughput of peer-to-peer communication links. Since SDMA arrangements do not require additional time- or frequency-slots, their spectrum efficiency is directly enhanced by this scheme.

D. Beamforming

In a beamforming scheme [40]–[43], half-wavelength spaced antenna elements are used to create an angularly selective filtering pattern, potentially at both the receivers and/or transmitters. The beamforming pattern based on *a priori* knowledge of the Directions-of-Departure (DODs) or Directions-of-Arrival (DOAs) results in achieving the beamforming gain, directly increasing the corresponding Signal-to-Noise Ratio (SNR). This also indicates an increase in the maximum communication range as well as a reduction of the ISI and flat fading. Furthermore, when a beamforming antenna array is employed at the receiver, multiple signals originating from different sources can be separated by the angular filtering, i.e. co-channel interference nulling, based on the user-specific DOAs. However, when the users' DODs or DOAs are close, this angular filtering capability is severely deteriorated, since its filtering resolution is determined by the antenna beamwidth of the array pattern, which is determined by the number of array elements.

E. Diversity Versus Multiplexing Tradeoff

In contrast to V-BLAST which is capable of achieving a high multiplexing gain, the class of STBCs is used to combat fading channels based on the concept of spatial diversity. However, it is not necessary to use the AEs purely either for multiplexing or for diversity. To be more specific, some of the space-time dimensions can be used for achieving a diversity gain, while the remaining dimensions may be used for attaining a multiplexing gain. According to the tutorial paper by Zheng and Tse [44], given a certain number of AEs, there is fundamental limitation regarding the achievable diversity-multiplexing gain tradeoff. This indicates that the degree of freedom in a MIMO system is determined by the number of AEs, which should be appropriately dedicated to each of the gains in MIMO systems so as to make the best use of the MIMO's capability. More explicitly, a system is capable of achieving an r -fold spatial multiplexing, when the data rate $R(\text{SNR})$ at a certain SNR value satisfies $\lim_{\text{SNR} \rightarrow \infty} R(\text{SNR})/\log_2 \text{SNR} = r$, while the diversity gain may be defined in terms of the achievable BER improvement as $\lim_{\text{SNR} \rightarrow \infty} \log P_e(\text{SNR})/\log \text{SNR} = -d$, where $P_e(\text{SNR})$ represents the average error probability. It was shown in [44] that if the number of symbol durations T per space-time block satisfies the relationship of $T \geq M + N - 1$, then we have [44] $d(r) = (M - r)(N - r)$, where we have $0 \leq r \leq \min(M, N)$.

The recent MIMO studies revealed that some combinations of the four MIMO techniques allow us to simultaneously exploit several MIMO functions [9], [45]–[49]. To elaborate a little further, the degree of freedom provided by multiple antennas can be allocated to achieve diversity, multiplexing and beamforming gains for the sake of enhancing robustness against fading, for increasing the data rates and/or for reducing

TABLE I
CONTRIBUTIONS TO DIVERSITY VERSUS MULTIPLEXING TRADEOFFS AND RELATED TECHNIQUES

Year	Authors	Contribution
1999	Tarokh <i>et al.</i> [45]	STBC and V-BLAST were combined in order to exploit both space-time diversity as well as multiplexing gains.
2002	Hassibi and Hochwald [9]	Proposed the achievable LDCs which are capable of striking a flexible tradeoff between diversity and multiplexing gain.
	Hassibi and Hochwald [46]	Proposed a differentially-encoded LDC architecture combined with PAM, which is based on the Cayley unitary transform technique.
	Jongren <i>et al.</i> [47]	Combined the benefits of conventional transmit beamforming and of orthogonal STBCs, assuming that the transmitter has partial knowledge of the channels.
2003	Zheng and Tse [44]	Characterized the MIMO's fundamental tradeoff between diversity and multiplexing gains.
2004	Tao and Cheng [48]	Proposed a generalized layered space-time code as an extension of [45], where the optimal serial decoding order was derived in order to improve the performance.
2005	Heath and Paulraj [51]	Proposed switching between spatial multiplexing and transmit diversity as a simple way to improve the diversity performance of spatial multiplexing.
2006	El Gamal <i>et al.</i> [52]	Explored the fundamental performance tradeoff of the delay-limited MIMO automatic retransmission request (ARQ) channel.
2007	El-Hajjar and Hanzo [53]	Presented the capacity analysis of a multi-functional MIMO system that combines the benefits of V-BLAST, STBC and beamforming.
2008	Sezgin <i>et al.</i> [54]	Studied an LDC system combined with transmitter preprocessing and a linear MMSE detector operating in a Ricean flat-fading environment.
2009	Wu and Hanzo [55]	Proposed irregular-precoded LDCs, while deriving the DCMC capacity of LDCs.
2010	Sugiura <i>et al.</i> [56], [57]	Proposed a Space-Time Shift Keying (STSK) philosophy, which is capable of striking a flexible rate-diversity tradeoff, while imposing no ICI at the receiver.

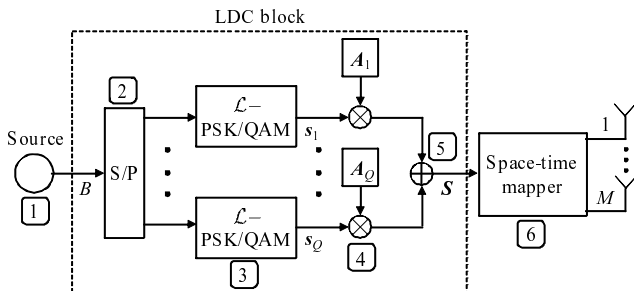


Fig. 2. Transmitter structure of our coherent LDC scheme.

the interference, respectively. A range of major contributions on the subject of diversity versus multiplexing tradeoffs and related techniques are listed in Table I.²

Linear Dispersion Codes: Hassibi and Hochwald [9] developed a sophisticated MIMO space-time processing architecture referred to as Linear Dispersion Codes (LDCs), which amalgamate the benefits of STC and SDM. The LDC was designed for striking a flexible diversity-multiplexing gain tradeoff for an arbitrary number of transmit and receive antennas, when using diverse modulation constellation sizes [9], [58]. As depicted in Fig. 2, at the LDC transmitter, Q independently modulated symbols $\mathbf{K} = [s_1, s_2, \dots, s_Q]^T \in \mathcal{C}^{Q \times 1}$ are mapped to the space-time block \mathbf{S} as follows: with the aid of a set of dispersion matrices $\mathbf{A}_q \in \mathcal{C}^{M \times Q}$ ($q = 1, \dots, Q$),

which are prepared prior to the commencement of transmissions. Here, the dispersion matrices \mathbf{A}_q are constructed using a certain criterion, such as the maximization of either the achievable diversity order [9] or of the channel capacity [55], while maintaining the power constraints of $\text{tr}[\mathbf{A}_q \mathbf{A}_q^H] = T/Q$ ($q = 1, \dots, Q$), leading to a unity transmission power per symbol duration. It can be seen from Eq. (1) that Q symbols $\mathbf{K} = [s_1, s_2, \dots, s_Q]^T$ are dispersed into both the M -spatial and T -time dimensions, generating $(M \times T)$ space-time codewords \mathbf{S} .³ To expound a little further, the LDCs having specific dispersion-matrix structure exhibits the arrangement equivalent to OSTBCs, BLAST, and so on [50].

II. SPACE-TIME SHIFT KEYING CONCEPT

In this section we present a simple and powerful Spatial Modulation (SM) scheme. Then, we introduce the unified STSK framework, where the SM concept is extended to both the time- and space-dimensions.

A. Spatial Modulation/Space-Shift Keying

Recently, Mesleh *et al.* [59], [60] proposed the sophisticated concept of SM, which serves as a novel MIMO encoding principle, which is fundamentally different from that of the SDM scheme. In the SM scheme, the transmitter activates one out of M transmit AEs, whose antenna-activation process acts

²For a list of other diverse MIMO-related development milestones, such as those in spatial diversity, differential spatial diversity, spatial multiplexing and cooperative MIMO techniques, please refer to in Chapter 1 of [50].

³By appropriately designing a set of dispersion matrices, the LDC scheme is capable of operating in an arbitrary transmit- and receive-antenna configuration, given the desirable transmission rate and achievable diversity order. Hence, the system parameters are fully characterized by the dispersion-matrix set employed.

$$\underbrace{\begin{bmatrix} t_{11} & \cdots & t_{1T} \\ \vdots & \ddots & \vdots \\ t_{M1} & \cdots & t_{MT} \end{bmatrix}}_{\mathbf{S}} = s_1 \underbrace{\begin{bmatrix} a_{11}^{(1)} & \cdots & a_{1T}^{(1)} \\ \vdots & \ddots & \vdots \\ a_{M1}^{(1)} & \cdots & a_{MT}^{(1)} \end{bmatrix}}_{\mathbf{A}_1} + \cdots + s_Q \underbrace{\begin{bmatrix} a_{11}^{(Q)} & \cdots & a_{1T}^{(Q)} \\ \vdots & \ddots & \vdots \\ a_{M1}^{(Q)} & \cdots & a_{MT}^{(Q)} \end{bmatrix}}_{\mathbf{A}_Q}, \quad (1)$$

TABLE II
EXAMPLE OF SM SCHEME EMPLOYING $M = 4$ TRANSMIT ANTENNAS,
MAPPING 3 BITS PER BLOCK, WITH THE AID OF BPSK CONSTELLATION

Input bits m, l	Antenna index $\#m$	BPSK symbol s_l
00 0	#1	+1
00 1	#1	-1
01 0	#2	+1
01 1	#2	-1
10 0	#3	+1
10 1	#3	-1
11 0	#4	+1
11 1	#4	-1

as an additional means of conveying information bits, and then only the activated antenna transmits a signal modulated with the aid of the classic \mathcal{L} -point constellation, such as PSK and Quadrature Amplitude Modulation (QAM). Unlike BLAST, SM schemes do not transmit simultaneously via M AEs, hence single-antenna based low-complexity ML detection can be employed at the receiver, while dispensing with symbol-level Inter-Antenna Synchronization (IAS) at the transmitter. A special case of SM is constituted by the scenario, where we deactivate the classic PSK/QAM signaling and simply use the presence or absence of energy assigned to a specific antenna, which is also referred to as Space Shift Keying (SSK) [61]. The SM/SSK philosophy was investigated in both uncoded [59]–[62] and channel-encoded scenarios [63]–[65], while the optimal ML detector designed for the uncoded SM/SSK scheme was presented in [61]. Although SM/SSK has the potential of outperforming other MIMO arrangements [59]–[61], [64], SM/SSK was not designed for achieving any transmit diversity gain and hence has to rely on the provision of receive diversity in order to combat the effects of fading channels.

In the above-mentioned conventional MIMO schemes, the source information is first modulated onto complex-valued symbols with the aid of classic modulation schemes, such as PSK and QAM, and then the modulated symbols are allocated to or dispersed to a space-time matrix \mathbf{S} . By contrast, the so-called SM/SSK scheme [59]–[61], [64] is based on a new modulation criterion, namely the activation of one out of a total of M antenna elements during each symbol interval. This leads to an additional means of conveying source information, while removing the effects of ICI.⁴ More specifically, let us assume having $B = \log_2(\mathcal{L} \cdot M) = \log_2 \mathcal{L} + \log_2 M$ input

⁴Since our STSK scheme, which will be proposed in this chapter, is inspired by and partly based on the SM/SSK concept, it is useful to revisit the encoding and decoding principle of the SM/SSK scheme.

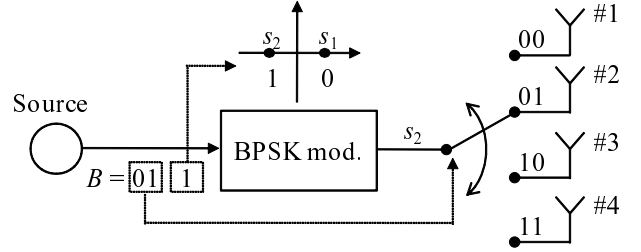


Fig. 3. SM mapping example, where binary bits of 011 are input to the BPSK-modulated SM employing $M = 4$ transmit antenna elements.

bits per block. Then the modulated signals $\mathbf{S}_{m,l} \in \mathcal{C}^{M \times 1}$ are represented by⁵

$$\mathbf{S}_{m,l} = \underbrace{[0, \dots, 0]_{m-1}}_{m-1}, s_l, \underbrace{[0, \dots, 0]_{M-m}}_{M-m}, \quad (2)$$

where s_l ($1 \leq l \leq \mathcal{L}$) represents the PSK/QAM symbol modulated according to the $\log_2 \mathcal{L}$ input bits, while the integer m ($1 \leq m \leq M$) corresponds to the rest of the input bits, i.e. the $\log_2 M$ bits. According to [59]–[61], [64], it is normally assumed that the number of transmit antennas M is set to 2^ι , where ι is an integer value. Note that this restriction may make it challenging to implement SM/SSK schemes for an arbitrary number of transmit antennas M . Considering that the number of symbol durations T per block is set to $T = 1$, the normalized transmission rate $R_{\text{SM/SSK}}$ of the SM/SSK scheme is written as $R_{\text{SM/SSK}} = \log_2(\mathcal{L} \cdot M)$ bits/symbol. It can be seen from Eq. (2) that since only one out of M antenna elements is activated during each symbol interval, symbol-level synchronization between the antenna elements is no longer needed. This allows us to avoid the elaborate calibration of the antenna-array.

To expound a little further, we exemplify the BPSK-modulated ($\mathcal{L} = 2$) SM/SSK modulation employing $M = 4$ transmit antennas in Table II and Fig. 3. As seen in Table II, $B = 3$ input bits are divided into two bits and one bit, and then the first two bits determine the activated antenna element (#1, #2, #3, #4), while the last single bit generates the BPSK symbol s_l ($l = 1, 2$). When binary symbols of “011” are input as shown in Fig. 3, the second antenna #2 is activated, while the second constellation point s_2 is selected as the transmitted symbol, according to the mapping rule seen in Table II.

Furthermore, this SM/SSK arrangement allows the employment of low-complexity single-antenna-based ML detection at

⁵As noted in [64], the SSK scheme can be viewed as the special case of the SM, where only the presence and absence of the energy assigned to each antenna element differentiates the transmitted information. More specifically, in the SSK scheme the activated antenna element only transmits a symbol of $s_1 = +1$, which may be considered to be $\mathcal{L} = 1$ -case of the SM scheme.

the receiver, while the BLAST scheme requires the potentially excessive-complexity joint detection of multiple antennas' signals. It is worth mentioning that upon increasing the number of transmit antennas M , the computational complexity required for this single-antenna-based ML detection increases linearly, while that of BLAST increases exponentially [61]. To be specific, the computational complexity per bit, evaluated in terms of the number of real-valued multiplications, is given by $6MN\mathcal{L}/\log_2(M \cdot \mathcal{L})$. This advantage becomes even more dominant in a rank-deficient scenario, where the number of transmit antennas is higher than that of the receive antennas and hence either an excessive complexity or a substantial performance degradation is imposed on SDM. As a result, it was demonstrated in [59]–[61], [64] that SM has the potential of outperforming other MIMO arrangements, such as BLAST and Alamouti's STBC schemes in some scenarios.

On the other hand, since SM adopted V-BLAST's high-rate architecture, which was designed for achieving a high rate, rather than diversity gain, it has to rely on the employment of multiple DL receive AEs for the sake of combating the effects of fading channels. However, accommodating multiple DL elements imposes challenges, when transmitting to mobiles in DL scenarios. Additionally, when aiming for a linear increase in the transmission rate, the number of transmit antennas employed in the context of [59]–[61], [64] has to be increased exponentially. Additionally, in [66] the employment of an arbitrary number of transmit antennas M was proposed, rather than obeying $M = 2^k$, where k is an integer.⁶

B. Space-Time Shift Keying Modulation Concept

As aforementioned, the recently-proposed SM/SSK scheme of Fig. 3 is based on the concept that source information is assigned to the spatial indices, i.e. to the transmit antennas, where only the spatial dimension is utilized for the classic modulation scheme and hence no transmit diversity gain is achieved. Considering the fact that the LDC scheme is capable of striking a flexible tradeoff between diversity and multiplexing gains by making the best use of both the spatial and time dimensions, it might be useful to extend the SM/SSK scheme so that both these two dimensions can be utilized. To this end, in this section we propose the so-called STSK modulation scheme, whose merits are listed as follows:

- The STSK scheme is capable of striking an attractive tradeoff between the achievable diversity gain and the high rate, by invoking the SM/SSK scheme of Fig. 3. Hence, our STSK scheme is capable of achieving both transmit as well as receive diversity gains, unlike the conventional SM and SSK schemes, which can only attain receive diversity gain.
- Since no ICI is imposed by the resultant equivalent system model of the STSK scheme, the employment of single-stream-based ML detection becomes realistic.

⁶More recently, another useful technique of providing a beneficial transmit diversity gain for SM/SSK schemes was presented in [67], where antenna-specific time-orthogonal pulse waveforms, such as Ultra-Wide Bandwidth (UWB) pulses [68], were invoked. Owing to the good auto- and cross-correlation properties of the pulse waveforms employed, the maximum achievable transmit diversity order of M may indeed be attained.

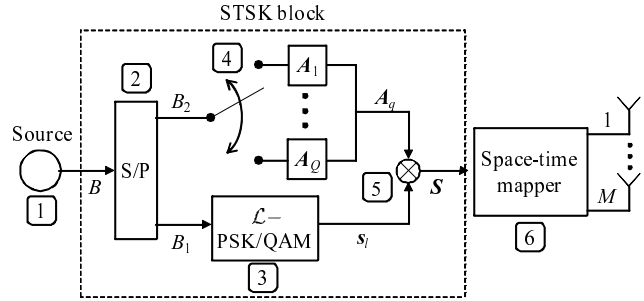


Fig. 4. Transmitter structure of our coherent STSK scheme.

- The STSK scheme can be configured to support asynchronous MIMO transmissions, which does not necessitate symbol-level IAS, similarly to the SM/SSK scheme.
- The STSK is capable of supporting an arbitrary transmit- and receive-antenna configuration, without any substantial information loss.

More specifically, the STSK scheme is based on the activation of Q number of appropriately indexed space-time dispersion matrices within each STSK block duration, rather than that of the indexed antennas at each symbol duration, as in the SM scheme of [59]–[61], [64].

Fig. 4 depicts the transmitter structure of our coherent STSK scheme, where Q dispersion matrices $\mathbf{A}_{q'} \in \mathcal{C}^{M \times T}$ ($q' = 1, \dots, Q$) are pre-assigned in advance of any transmission. A total of $B = \log_2(Q \cdot \mathcal{L})$ source bits are mapped to each space-time block $\mathbf{S} \in \mathcal{C}^{M \times T}$ by the STSK scheme of Fig. 4, where s_l is the complex-valued symbol of the conventional modulation scheme employed, such as \mathcal{L} -PSK or \mathcal{L} -QAM, which is associated with $B_1 = \log_2 \mathcal{L}$ number of input bits. By contrast, the specific matrix \mathbf{A}_q is selected from the Q dispersion matrices $\mathbf{A}_{q'}$ ($q' = 1, \dots, Q$) according to $B_2 = \log_2 Q$ number of input bits. Additionally, in order to maintain a unity average transmission power for each STSK symbol duration, each of the Q dispersion matrices has to obey the power constraint of $\text{tr}[\mathbf{A}_{q'}^H \mathbf{A}_{q'}] = T$ ($q' = 1, \dots, Q$), where $\text{tr}[\cdot]$ indicates the trace operation. Note that this power constraint is Q times higher than that of LDC in Section I-E, since the LDC scheme linearly combines the Q dispersion matrices, while our STSK activates only one out of them.

In this way, an additional means of transmitting further information bits was created. To be specific, we exemplify in Table III the mapping rule of our STSK modulation scheme, where a fixed number of $B = \log_2(Q \cdot \mathcal{L}) = 3$ bits per space-time block \mathbf{S} are transmitted by employing \mathcal{L} -PSK, for the specific cases of $(Q, \mathcal{L}) = (1, 8; 2, 4; 4, 2; 8, 1)$. As seen from Table III, there are several possible combinations of the number of dispersion matrices Q and of the constellation size \mathcal{L} , given a total throughput of 3 source bits per space-time block. For example, assume that the information bits “101” are input to our STSK scheme employing QPSK modulation ($\mathcal{L} = 4$) and $Q = 2$. Then, according to Table III we arrive at the modulated space-time block of $\mathbf{S} = s_2 \mathbf{A}_2 = e^{j\frac{\pi}{4}} \mathbf{A}_2$.

Moreover, the normalized throughput per time-slot (or per symbol) R of our STSK scheme may be expressed as $R = \log_2(Q \cdot \mathcal{L})/T$ [bits/symbol]. In the rest of this chapter, we employ the parameter-based notation of our STSK scheme

$$\begin{aligned}
\mathbf{S} &= s_l \mathbf{A}_q \\
&= 0 \underbrace{\begin{bmatrix} a_{11}^{(1)} & \cdots & a_{1T}^{(1)} \\ \vdots & \ddots & \vdots \\ a_{M1}^{(1)} & \cdots & a_{MT}^{(1)} \end{bmatrix}}_{\mathbf{A}_1} + \cdots + 0 \underbrace{\begin{bmatrix} a_{11}^{(q-1)} & \cdots & a_{1T}^{(q-1)} \\ \vdots & \ddots & \vdots \\ a_{M1}^{(q-1)} & \cdots & a_{MT}^{(q-1)} \end{bmatrix}}_{\mathbf{A}_{q-1}} \leftarrow \left(\begin{array}{c} \text{deactivated} \\ \text{matrices} \end{array} \right) \\
&\quad + s_l \underbrace{\begin{bmatrix} a_{11}^{(q)} & \cdots & a_{1T}^{(q)} \\ \vdots & \ddots & \vdots \\ a_{M1}^{(q)} & \cdots & a_{MT}^{(q)} \end{bmatrix}}_{\mathbf{A}_q} \leftarrow \left(\begin{array}{c} \text{activated} \\ \text{matrix} \end{array} \right) \\
&\quad + 0 \underbrace{\begin{bmatrix} a_{11}^{(q+1)} & \cdots & a_{1T}^{(q+1)} \\ \vdots & \ddots & \vdots \\ a_{M1}^{(q+1)} & \cdots & a_{MT}^{(q+1)} \end{bmatrix}}_{\mathbf{A}_{q+1}} + \cdots + 0 \underbrace{\begin{bmatrix} a_{11}^{(Q)} & \cdots & a_{1T}^{(Q)} \\ \vdots & \ddots & \vdots \\ a_{M1}^{(Q)} & \cdots & a_{MT}^{(Q)} \end{bmatrix}}_{\mathbf{A}_Q}, \leftarrow \left(\begin{array}{c} \text{deactivated} \\ \text{matrices} \end{array} \right) \quad (3)
\end{aligned}$$

TABLE III
EXAMPLE OF STSK MODULATION SCHEME, MAPPING 3 BITS PER SPACE-TIME BLOCK, WITH THE AID OF \mathcal{L} -PSK CONSTELLATION

Input bits	$Q = 1$ $\mathcal{L} = 8$		$Q = 2$ $\mathcal{L} = 4$		$Q = 4$ $\mathcal{L} = 2$		$Q = 8$ $\mathcal{L} = 1$	
	\mathbf{A}_q	s_l	\mathbf{A}_q	s_l	\mathbf{A}_q	s_l	\mathbf{A}_q	s_l
000	\mathbf{A}_1	$s_1 = 1$	\mathbf{A}_1	$s_1 = 1$	\mathbf{A}_1	$s_1 = 1$	\mathbf{A}_1	$s_1 = 1$
001	\mathbf{A}_1	$s_2 = e^{j\frac{\pi}{4}}$	\mathbf{A}_1	$s_2 = e^{j\frac{\pi}{2}}$	\mathbf{A}_1	$s_2 = e^{j\pi}$	\mathbf{A}_2	$s_1 = 1$
010	\mathbf{A}_1	$s_3 = e^{j\frac{2\pi}{4}}$	\mathbf{A}_1	$s_3 = e^{j\frac{2\pi}{2}}$	\mathbf{A}_2	$s_1 = 1$	\mathbf{A}_3	$s_1 = 1$
011	\mathbf{A}_1	$s_4 = e^{j\frac{3\pi}{4}}$	\mathbf{A}_1	$s_4 = e^{j\frac{3\pi}{2}}$	\mathbf{A}_2	$s_2 = e^{j\pi}$	\mathbf{A}_4	$s_1 = 1$
100	\mathbf{A}_1	$s_5 = e^{j\frac{4\pi}{4}}$	\mathbf{A}_2	$s_1 = 1$	\mathbf{A}_3	$s_1 = 1$	\mathbf{A}_5	$s_1 = 1$
101	\mathbf{A}_1	$s_6 = e^{j\frac{5\pi}{4}}$	\mathbf{A}_2	$s_2 = e^{j\frac{\pi}{2}}$	\mathbf{A}_3	$s_2 = e^{j\pi}$	\mathbf{A}_6	$s_1 = 1$
110	\mathbf{A}_1	$s_7 = e^{j\frac{6\pi}{4}}$	\mathbf{A}_2	$s_3 = e^{j\frac{2\pi}{2}}$	\mathbf{A}_4	$s_1 = 1$	\mathbf{A}_7	$s_1 = 1$
111	\mathbf{A}_1	$s_8 = e^{j\frac{7\pi}{4}}$	\mathbf{A}_2	$s_4 = e^{j\frac{3\pi}{2}}$	\mathbf{A}_4	$s_2 = e^{j\pi}$	\mathbf{A}_8	$s_1 = 1$

formulated as $\text{STSK}(M, N, T, Q)$ for ease of treatment.

To elaborate a little further, our STSK scheme includes the SM arrangement as its special case. For example, it is readily seen that $\text{STSK}(2, N, 1, 2)$ employing $\mathbf{A}_1 = [1 \ 0]^T$ and $\mathbf{A}_2 = [0 \ 1]^T$ is equivalent to the SM scheme assisted by $M = 2$ transmit antennas [60]. Again, since in our STSK scheme the source bits are mapped to both the space and time-domain, rather than only to the spatial domain of the SM scheme [59]–[61], [64], the SM arrangement is included in our STSK scheme associated with $T = 1$, where mapping to the time dimension was deactivated. It should also be noted that while SM has to exponentially increase the number of transmit AEs for the sake of linearly increasing the number of transmitted input bits, our STSK scheme may circumvent this problem by increasing the number of dispersion matrices Q . Therefore, given an affordable tradeoff in terms of number of transmit antennas M , our STSK scheme is capable of optimizing the derived transmission rate and diversity order in a more flexible and efficient manner by appropriately choosing T and Q .

Following the above-mentioned introductory elaborations on the STSK transmitter's encoding operation obeying the

architecture of Fig. 4, each of the steps numbered in the figure may be summarized as follows:

Algorithm 1: Encoding principle of the STSK's transmitter of Fig. 4

- 1) Given the \mathcal{L} -PSK/QAM CSTSK(M, N, T, Q) scheme, $B = \log_2(Q \cdot \mathcal{L})$ information bits are input to the STSK block in each of the Space-Time (ST) block durations T .
- 2) The $B = \log_2(Q \cdot \mathcal{L})$ information bits are Serial-to-Parallel (S/P) converted to $B_1 = \log_2 \mathcal{L}$ bits and $B_2 = \log_2 Q$ bits.
- 3) The $B_1 = \log_2 \mathcal{L}$ bits at the lower output of the S/P converter of Fig. 4 are then modulated to a complex-valued \mathcal{L} -PSK/QAM symbol $\{s_l; l = 1, \dots, \mathcal{L}\}$.
- 4) According to the $B_2 = \log_2 Q$ bits at the lower output of the S/P converter of Fig. 4, one out of the Q dispersion matrices $\mathbf{A}_1, \dots, \mathbf{A}_Q \in \mathcal{C}^{M \times T}$ is chosen, which we refer to as the activated matrix $\{\mathbf{A}_q; q = 1, \dots, Q\}$.
- 5) According to the modulated symbol s_l generated in Step 3 as well as the dispersion matrix \mathbf{A}_q activated in Step 4, a ST matrix $\mathbf{S} \in \mathcal{C}^{M \times T}$ is calculated as follows: $\mathbf{S} = s_l \cdot \mathbf{A}_q$.

- 6) The space-time matrix \mathbf{S} generated in *Step 5* is then mapped to the space- and time-dimensions, where the specific component in the m th row and t th column of the matrix \mathbf{S} is assigned to the m th antenna element in the t th symbol duration.

Having formalized our CSTSK scheme's encoding algorithm, we then propose a modified CSTSK structure in the following section.

C. Asynchronous STSK Modulation

Additionally, we introduce an improved STSK structure, which enables us to dispense with any symbol-level time-synchronization between the RF chains associated with the transmit AEs, similarly to the SM/SSK scheme. As mentioned in [59]–[61], [64], the SM and SSK schemes do not require any symbol-level time synchronization between the transmit antenna circuits, because a single antenna is activated at each symbol instant in these schemes. By contrast, our STSK scheme introduced in the previous section, potentially requires IAS for the STSK's dispersion matrix activation, which replaces the antenna activation. However, by carefully designing the dispersion matrices $\mathbf{A}_{q'}$ ($q' = 1, \dots, Q$) of our STSK, we will contrive an ASTSK arrangement dispensing with any IAS. More specifically, the structure of each dispersion matrix $\mathbf{A}_{q'}$ is constructed so that there is a single non-zero element for each column of the dispersion matrix $\mathbf{A}_{q'}$. This constraint enables us to avoid any simultaneous transmission by multiple antennas, similarly to the conventional SM and SSK schemes, while retaining all the benefits of our STSK scheme.

For example, let us consider the ASTSK(3, N , 3, 4) system. Then a set of dispersion matrices $\mathbf{A}_{q'}$ ($q' = 1, 2, 3, 4$) may be given by Eq. (4), which is situated at the top of the following page. In each column of the four dispersion matrices $\mathbf{A}_1, \mathbf{A}_2, \mathbf{A}_3, \mathbf{A}_4$, there is only a single non-zero element, while the other two elements are set to 0s. Hence, this ASTSK arrangement indicates that regardless of the specific dispersion matrix activated in the STSK modulation process of Fig. 4, only one antenna element transmits a signal at any symbol instance. It should be noted that since the introduction of the ASTSK concept reduces the search space of the set of dispersion matrices, the achievable performance may be degraded in comparison to that of the STSK scheme, while the ASTSK's dispersion-matrix design also becomes less complex.

D. Optimal ML Detector for the Proposed STSK Scheme

Having generated the space-time block \mathbf{S} to be transmitted, we then introduce the ML detection algorithm of our STSK scheme. By applying the vectorial stacking operation $\text{vec}(\cdot)$ to the received signal block $\mathbf{Y} = \mathbf{H}\mathbf{S} + \mathbf{V}$, we arrive at the linearized equivalent system model formulated as follows: [58]

$$\bar{\mathbf{Y}} = \bar{\mathbf{H}}\chi\mathbf{K}_{q,l} + \bar{\mathbf{V}}, \quad (5)$$

with the relations of $\bar{\mathbf{Y}} = \text{vec}(\mathbf{Y}) \in \mathcal{C}^{NT \times 1}$, $\bar{\mathbf{H}} = \mathbf{I} \otimes \mathbf{H}(i) \in \mathcal{C}^{NT \times MT}$, $\bar{\mathbf{V}} = \text{vec}(\mathbf{V}) \in \mathcal{C}^{NT \times 1}$ and $\chi = [\text{vec}(\mathbf{A}_1) \cdots \text{vec}(\mathbf{A}_Q)] \in \mathcal{C}^{MT \times Q}$, where \mathbf{I} is the identity matrix and \otimes is the Kronecker product. Furthermore,

the equivalent transmitted signal vector $\mathbf{K}_{q,l} \in \mathcal{C}^{Q \times 1}$ is written as

$$\mathbf{K}_{q,l} = \underbrace{[0, \dots, 0]_{q-1}}_{q-1}, s_l, \underbrace{[0, \dots, 0]_{Q-q}}_{Q-q}, \quad (6)$$

where the modulated symbol s_l is situated in the q th element, noting that the index q corresponds to the index of the dispersion matrix \mathbf{A}_q activated during the corresponding STSK block. Therefore, the number of legitimate transmit signal vectors $\mathbf{K}_{q,l}$ is given by $Q \cdot \mathcal{L}$.

Since the equivalent system model of Eq. (5) is free from the effects of ICI, we can employ the single-antenna-based ML detector of [61], which imposes a low complexity. Let us consider that (q, l) correspond to the specific input bits of a STSK block, which are mapped to the l th ($l = 1, \dots, \mathcal{L}$) PSK/QAM symbol and q th ($q = 1, \dots, Q$) dispersion matrix. Then the estimates (\hat{q}, \hat{l}) are given by $(\hat{q}, \hat{l}) = \arg \min_{q,l} \|\bar{\mathbf{Y}} - \bar{\mathbf{H}}\chi\mathbf{K}_{q,l}\|^2 = \arg \min_{q,l} \|\bar{\mathbf{Y}} - s_l(\bar{\mathbf{H}}\chi)_q\|^2$, where s_l represents the l th symbol in the \mathcal{L} -point constellation. Furthermore, $(\bar{\mathbf{H}}\chi)_q$ is the q th column vector of the matrix $\bar{\mathbf{H}}\chi$. As mentioned in [61], this low-complexity ML detector exhibits the optimal detection performance in the uncoded scenario, where no *a priori* information is provided and the source bits are equi-probable.

E. Computational Complexity

Let us now characterize the computational complexity imposed by the ML detection of our STSK scheme, which is given by $NTQ[(4MT + 4\mathcal{L})/\tau + 2\mathcal{L}]/\log_2(Q \cdot \mathcal{L})$ [57], [69], where τ represents an integer, quantifying the coherence block interval in slow fading environments. Here, their complexity is evaluated in terms of the number of real-valued multiplications, noting that a single complex-valued multiplication was considered equivalent to four real-valued multiplications.⁷

Moreover, the computational complexity of the ASTSK receiver is further simplified into $NTQ[(4T + 4\mathcal{L})/\tau + 2\mathcal{L}]/\log_2(Q \cdot \mathcal{L})$, because each dispersion matrix of the ASTSK scheme is sparse and hence the complexity imposed by calculating $\bar{\mathbf{H}}\chi$ becomes lower than that of the STSK scheme by a factor of M . More specifically, the proposed STSK schemes have a substantially lower complexity ML receiver in comparison to classic MIMO schemes, such as V-BLAST and LDCs, which is an explicit benefit of our ICI-free system model.

Table IV summarizes the diversity gain/order, complexity and throughput of different MIMO schemes, where the complexity was evaluated in terms of the number of real-valued multiplications required for implementing ML detection at each scheme's detector.

III. UNIFIED SPACE-TIME ARCHITECTURE

In Section II, we introduced the new unified STSK MIMO modulation principle, which adopts the underlying concept of

⁷We acknowledge that there are several potential approaches, which can be used for assessing the decoding complexity. For example, we may consider both the number of real-valued multiplications as well as the number of additions as a measure of the decoding complexity, although one may argue that a d -bit multiplication requires d shift-and-add operations and hence may be deemed d -times more complex.

$$\mathbf{A}_1 = \begin{bmatrix} a_1^{(1)} & 0 & 0 \\ 0 & a_2^{(1)} & 0 \\ 0 & 0 & a_3^{(1)} \end{bmatrix}, \mathbf{A}_2 = \begin{bmatrix} 0 & 0 & a_3^{(2)} \\ a_1^{(2)} & 0 & 0 \\ 0 & a_2^{(2)} & 0 \end{bmatrix},$$

$$\mathbf{A}_3 = \begin{bmatrix} 0 & a_2^{(3)} & 0 \\ 0 & 0 & a_3^{(3)} \\ a_1^{(3)} & 0 & 0 \end{bmatrix}, \mathbf{A}_4 = \begin{bmatrix} 0 & a_2^{(4)} & 0 \\ a_1^{(4)} & 0 & 0 \\ 0 & 0 & a_3^{(4)} \end{bmatrix}, \quad (4)$$

TABLE IV
DIVERSITY, RATE AND COMPLEXITY FOR VARIOUS COHERENTLY-DETECTED MIMO ARRANGEMENTS, I.E. THE OSTBCS, THE SDM SCHEME, THE LDCs, THE SM/SSK SCHEME, THE STSK SCHEME AND THE ASTSK SCHEME.

Scheme	Section	Diversity	Complexity	Rate
OSTBC	Section I-A	$M \cdot N$	$\mathcal{O}\left(\frac{MN\mathcal{L}}{\log_2 \mathcal{L}}\right)$	$\leq \log_2 \mathcal{L}$
SDM	Section I-B	N	$\mathcal{O}\left(\frac{N\mathcal{L}^M}{\log_2 \mathcal{L}}\right)$	$M \log_2 \mathcal{L}$
LDC	Section I-E	$N \cdot \min(M, T)$	$\mathcal{O}\left(\frac{NT\mathcal{L}^Q}{\log_2 \mathcal{L}}\right)$	$Q \log_2 \mathcal{L}/T$
SM/SSK	Section II-A	N	$\mathcal{O}\left(\frac{MN\mathcal{L}}{\log_2(M \cdot \mathcal{L})}\right)$	$\log_2(M \cdot \mathcal{L})$
STSK	Section II-B	$N \cdot \min(M, T)$	$\mathcal{O}\left(\frac{MNT^2Q\mathcal{L}}{\log_2(Q \cdot \mathcal{L})}\right)$	$\log_2(Q \cdot \mathcal{L})/T$
ASTSK	Section II-C	$N \cdot \min(M, T)$	$\mathcal{O}\left(\frac{NT^2Q\mathcal{L}}{\log_2(Q \cdot \mathcal{L})}\right)$	$\log_2(Q \cdot \mathcal{L})/T$

activating one out of Q dispersion matrices, whose matrix-activation process acts as an additional means of conveying information bits. This STSK concept enables us to invoke a realistic single-stream-based ML detection, since no spatial multiplexing is used. Hence its multiplexing gain is unity. By contrast, as described in Section I-E, the classic LDC scheme may be viewed as another unified MIMO scheme, where all the Q preassigned dispersion matrices are linearly combined and the resultant multiplexed streams are transmitted simultaneously. Thus, the multiplexing gain of the LDC scheme corresponds to the value of Q , where the transmission rate can be linearly increased with Q at the cost of a substantially increased computational complexity.

Bearing in mind that both the STSK and LDC schemes are capable of striking flexible rate-multiplexing tradeoffs, a further generalized MIMO framework may be conceived by increasing the number of activated dispersion matrices in the STSK scheme, which amalgamates benefits of both the STSK scheme's dispersion-matrix activation as well as those of the LDC scheme's dispersed-symbol based multiplexing capability. The resultant arrangement is capable of achieving significantly flexible rate-, diversity- and complexity-tradeoffs. More specifically, in this chapter we will propose the so-called Generalized STSK (GSTSK) family, where P out of Q dispersion matrices are activated during each transmission interval. As shown in Fig. 5, owing to its high flexibility, the GSTSK framework subsumes most of the above-mentioned MIMO arrangements, such as SM/SSK, LDC, OSTBC as well as BLAST, and therefore has the potential of flexibly mimicking all of them. Additionally, we conceive the optimal ML detector designed for uncoded GSTSK systems and the soft-demodulator conceived for the coded GSTSK systems.

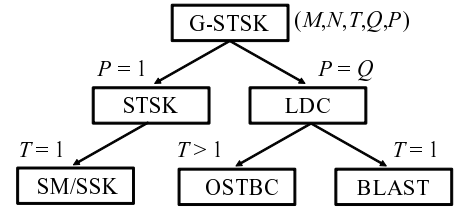


Fig. 5. Relationship between our GSTSK scheme and other MIMO schemes.

A. Generalized Space-Time Shift Keying Modulation

Fig. 6 shows the schematic of our GSTSK's transmitter. In the GSTSK bit-to-symbol mapping scheme, $B = \log_2 f(Q, P) + P \log_2 \mathcal{L}$ bits per block are mapped to a space-time codeword $\mathcal{S}(i)$, where $f(Q, P)$ is calculated from Q and P as $f(Q, P) = 2^\iota$, while the integer ι satisfies the following inequality $2^\iota \leq \binom{Q}{P} < 2^{\iota+1}$.⁸ Firstly, $B = \log_2 f(Q, P) + P \log_2 \mathcal{L}$ input bits are S/P converted to $B_1 = \log_2 f(Q, P)$ bits and $B_2 = P \log_2 \mathcal{L}$ bits. Then, at the dispersion-matrix activation block of Fig. 6, P out of Q pre-assigned dispersion matrices $\mathbf{A}_{q'} \in \mathcal{C}^{M \times T}$ ($q' = 1, \dots, Q$) are activated according to $B_1 = \log_2 f(Q, P)$ input bits, in order to have $\mathbf{A}^{(p)}(i)$ ($p = 1, \dots, P$). By contrast, according to $B_2 = P \log_2 \mathcal{L}$ input bits, P number of $\log_2 \mathcal{L}$ bits are separately modulated by the classic \mathcal{L} -point PSK/QAM modulation scheme, giving rise to the symbols $s^{(p)}(i)$ ($p = 1, \dots, P$).

⁸Although $f(Q, P)$ corresponds to P -out-of- Q dispersion-matrix selection process and can be given by $\binom{Q}{P}$ at maximum, this relationship restricts $\log_2 f(Q, P)$ to be a integer number for simplicity of the input-bit treatment.

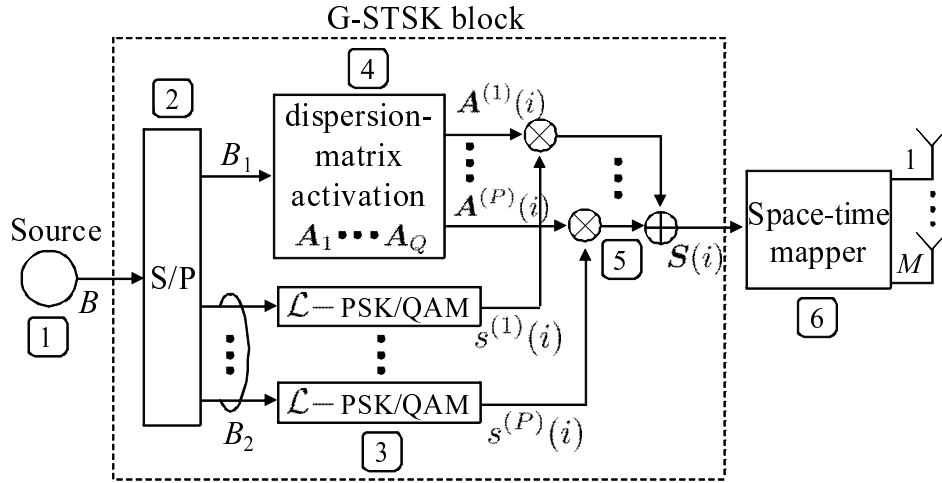


Fig. 6. Transmitter structure of our GSTSK scheme, which was developed from the STSK architecture of Fig. 4.

Finally, the space-time codeword $\mathbf{S}(i)$ is generated as follows:

$$\mathbf{S}(i) = \sum_{p=1}^P s^{(p)}(i) \mathbf{A}^{(p)}(i), \quad (7)$$

where we have the power constraint of $\text{tr}[\mathbf{A}_{q'} \mathbf{A}_{q'}^H] = T/P$ ($q' = 1, \dots, Q$), in order to maintain a unity total transmission power per symbol. Here, $\text{tr}[\cdot]$ represents the trace operation. We note that each of the P PSK/QAM symbols $s^{(p)}(i)$ is dispersed both to the M spatial and T time dimensions, with the aid of the activated dispersion matrices $\mathbf{A}^{(p)}(i)$.

Hence, our GSTSK scheme has a set of parameters given by M, N, T, Q and P . Therefore we employ the parameter-based system description of $\text{GSTSK}(M, N, T, Q, P)$ for simplicity. Additionally, the normalized throughput R of our GSTSK scheme is given by $R = B/T = \log_2 f(Q, P) + P \log_2 \mathcal{L}/T$ [bits/symbol].

To be more specific, in Table V we exemplify the bit-to-symbol mapping rule of BPSK-modulated ($\mathcal{L} = 2$) $\text{GSTSK}(M, N, T, 3, 2)$, where we have $f(Q, P) = 2^\ell = 2$. As seen in Table V, the $B = 4$ input bits are S/P converted to $B_1 = 2$ bits and $B_2 = 2$ bits. According to the B_1 bits, $P = 2$ out of $Q = 4$ dispersion matrices are selected as $\mathbf{A}^{(1)}(i), \mathbf{A}^{(2)}(i)$, while the B_2 bits generate the $P = 2$ BPSK symbols $s^{(1)}(i), s^{(2)}(i)$. Finally, the space-time codeword $\mathbf{S}(i)$ is generated as $\mathbf{S}(i) = s^{(1)}(i) \mathbf{A}^{(1)}(i) + s^{(2)}(i) \mathbf{A}^{(2)}(i)$.

Following the above-mentioned introductory elaborations, the encoding principle of our GSTSK scheme obeying the architecture of Fig. 6 can be formally summarized as follows: **Algorithm 2:**⁹ Encoding principle of the GSTSK's transmitter of Fig. 6

- 1) Given the \mathcal{L} -PSK/QAM aided $\text{GSTSK}(M, N, T, Q, P)$ scheme employing Q dispersion matrices $\mathbf{A}_1, \dots, \mathbf{A}_Q \in \mathcal{C}^{M \times T}$, $B = \log_2(Q \cdot \mathcal{L})$ information bits are input to the GSTSK block of Fig. 6 in each of the space-time block durations T .

- 2) The $B = \log_2(Q \cdot \mathcal{L})$ information bits, input in *Step 1*, are Serial-to-Parallel (S/P) converted to $B_1 = P \log_2 \mathcal{L}$ bits and $B_2 = \log_2 f(Q, P)$ bits, where $f(Q, P)$ satisfies the relation of $f(Q, P) = 2^\ell \leq \binom{Q}{P} < 2^{\ell+1}$.
- 3) The $B_1 = \log_2 \mathcal{L}$ bits at the lower output of the S/P converter of Fig. 6 are then modulated to P complex-valued \mathcal{L} -PSK/QAM symbols $s^{(p)}$ ($p = 1, \dots, P$).
- 4) According to the $B_2 = \log_2 Q$ bits at the upper output of the S/P converter of Fig. 6 as well as to the corresponding lookup table, P out of the Q dispersion matrices $\mathbf{A}^{(1)}, \dots, \mathbf{A}^{(P)} \in \mathcal{C}^{M \times T}$ are activated.
- 5) According to the modulated symbols $s^{(p)}$ ($p = 1, \dots, P$) generated in *Step 3* as well as to the dispersion matrices $\mathbf{A}^{(p)}$ ($p = 1, \dots, P$) activated in *Step 4*, a matrix $\tilde{\mathbf{S}} \in \mathcal{C}^{M \times T}$ is computed as follows: $\tilde{\mathbf{S}} = \sum_{p=1}^P s^{(p)} \cdot \mathbf{A}^{(p)}$.
- 6) The ST matrix \mathbf{S} generated in *Step 5* is mapped to the space- and time-dimensions, where the components in the m th row and t th column of the matrix \mathbf{S} are assigned to the m th antenna element in the t th symbol duration.

B. GSTSK Versus Conventional MIMO Arrangements

Next, we will demonstrate that our GSTSK scheme of Fig. 6 includes diverse MIMO arrangements.

1) *Spatial Modulation/Space-Shift Keying*: The conventional SM/SSK schemes [59]–[61], [64] of Section II-A may be derived by the $\text{GSTSK}(M, N, 1, Q = M, 1)$ scheme of Fig. 6 employing the dispersion matrices of

$$\mathbf{A}_1 = \begin{bmatrix} 1 \\ 0 \\ \vdots \\ 0 \end{bmatrix}, \mathbf{A}_2 = \begin{bmatrix} 0 \\ 1 \\ \vdots \\ 0 \end{bmatrix}, \dots, \mathbf{A}_Q = \begin{bmatrix} 0 \\ 0 \\ \vdots \\ 1 \end{bmatrix}, \quad (8)$$

where the number of dispersion matrices Q is set to the number of the transmit antennas M . As also seen in Section II-A, SM/SSK was not designed for exploiting any transmit diversity, due to the constraint of $T = 1$.

⁹Readers who are interested in further details can refer to [56], [57], [70] for the STSK scheme and to [70]–[72] for the GSTSK scheme.

TABLE V
EXAMPLE OF GSTSK(2, 2, 2, 4, 2) MODULATION SCHEME OF FIG. 6, MAPPING $B = 4$ BITS PER SPACE-TIME BLOCK, WITH THE AID OF BPSK CONSTELLATION

input bits $B = 4$		dispersion matrices	BPSK symbols	space-time codeword
$B_1=2$	$B_2=2$	$\mathbf{A}^{(1)}(i), \mathbf{A}^{(2)}(i)$	$s^{(1)}(i), s^{(2)}(i)$	$\mathbf{S}(i)$
00	00	$\mathbf{A}_1, \mathbf{A}_2$	+1, +1	$\mathbf{A}_1 + \mathbf{A}_2$
00	01	$\mathbf{A}_1, \mathbf{A}_2$	+1, -1	$\mathbf{A}_1 - \mathbf{A}_2$
00	10	$\mathbf{A}_1, \mathbf{A}_2$	-1, +1	$-\mathbf{A}_1 + \mathbf{A}_2$
00	11	$\mathbf{A}_1, \mathbf{A}_2$	-1, -1	$-\mathbf{A}_1 - \mathbf{A}_2$
01	00	$\mathbf{A}_1, \mathbf{A}_3$	+1, +1	$\mathbf{A}_1 + \mathbf{A}_3$
01	01	$\mathbf{A}_1, \mathbf{A}_3$	+1, -1	$\mathbf{A}_1 - \mathbf{A}_3$
01	10	$\mathbf{A}_1, \mathbf{A}_3$	-1, +1	$-\mathbf{A}_1 + \mathbf{A}_3$
01	11	$\mathbf{A}_1, \mathbf{A}_3$	-1, -1	$-\mathbf{A}_1 - \mathbf{A}_3$
10	00	$\mathbf{A}_2, \mathbf{A}_4$	+1, +1	$\mathbf{A}_2 + \mathbf{A}_4$
10	01	$\mathbf{A}_2, \mathbf{A}_4$	+1, -1	$\mathbf{A}_2 - \mathbf{A}_4$
10	10	$\mathbf{A}_2, \mathbf{A}_4$	-1, +1	$-\mathbf{A}_2 + \mathbf{A}_4$
10	11	$\mathbf{A}_2, \mathbf{A}_4$	-1, -1	$-\mathbf{A}_2 - \mathbf{A}_4$
11	00	$\mathbf{A}_3, \mathbf{A}_4$	+1, +1	$\mathbf{A}_3 + \mathbf{A}_4$
11	01	$\mathbf{A}_3, \mathbf{A}_4$	+1, -1	$\mathbf{A}_3 - \mathbf{A}_4$
11	10	$\mathbf{A}_3, \mathbf{A}_4$	-1, +1	$-\mathbf{A}_3 + \mathbf{A}_4$
11	11	$\mathbf{A}_3, \mathbf{A}_4$	-1, -1	$-\mathbf{A}_3 - \mathbf{A}_4$

2) *Linear Dispersion Code*: According to the system model of [58], our GSTSK framework associated with $P = Q$ has an identical system model to that of LDCs reviewed in Section I-E and in Fig. 2, where all of the Q pre-assigned dispersion matrices are used for the linear space-time dispersion of classic PSK/QAM symbols.

3) *Orthogonal Space-Time Block Code*: A class of Orthogonal STBCs (OSTBCs) [4], [5] is also subsumed by the GSTSK scheme of Fig. 6 upon setting $P = Q$ and using appropriately designed dispersion matrices, depending on the space-time codewords employed. For example, consider an $(M \times N) = (2 \times 2)$ QPSK-modulated Alamouti STBC [4]. Then the space-time codeword $\mathbf{S}(i)$ of Eq. (7) may be expressed as

$$\begin{aligned} \mathbf{S}(i) &= \frac{1}{\sqrt{2}} \begin{bmatrix} s_1 & s_2 \\ -s_2^* & s_1^* \end{bmatrix} \\ &= \underbrace{\begin{bmatrix} \frac{1}{2} & 0 \\ 0 & \frac{1}{2} \end{bmatrix}}_{\mathbf{A}_1} \sqrt{2}\alpha_1 + j \underbrace{\begin{bmatrix} \frac{1}{2} & 0 \\ 0 & -\frac{1}{2} \end{bmatrix}}_{\mathbf{A}_2} \sqrt{2}\beta_1 \\ &\quad + \underbrace{\begin{bmatrix} 0 & \frac{1}{2} \\ -\frac{1}{2} & 0 \end{bmatrix}}_{\mathbf{A}_3} \sqrt{2}\alpha_2 + j \underbrace{\begin{bmatrix} 0 & \frac{1}{2} \\ \frac{1}{2} & 0 \end{bmatrix}}_{\mathbf{A}_4} \sqrt{2}\beta_2, \end{aligned}$$

where $s_1 = \alpha_1 + j\beta_1$ and $s_2 = \alpha_2 + j\beta_2$ are two consecutive QPSK symbols per transmission block. From this relationship, we may regard the QPSK-modulated Alamouti code as a BPSK-modulated GSTSK(2, 2, 2, 4, 4) arrangement, employing $\mathbf{A}_{q'}$ ($q' = 1, \dots, 4$). In the same manner, the space-time codeword $\mathbf{S}(i)$ of G₃-OSTBC [14] can be represented by Eq. (9), which is shown at the top of the following page, where $s_i = \alpha_i + j\beta_i$ ($i = 1, 2, 3$) represents three QPSK symbols per block. Hence, it can be inferred from Eq. (9) that QPSK-modulated G₃-OSTBC may be viewed as the

BPSK-modulated GSTSK(3, N , 4, 6, 6) scheme. By following a similar decomposition process, other OSTBCs may also be represented by our GSTSK system. Moreover, it may be readily shown that other STBCs, such as Quasi-OSTBCs (QOSTBCs), STBC employing Time Variant Linear Transformation (TVLT) and Threaded Algebraic STBCs (TASTBCs), are also described by our GSTSK structure, according to Section 7.3 of [50]. Here, the STBCs are designed so as to remain unaffected by ICI and to achieve a full transmit diversity, which is achieved at the cost of sacrificing the achievable multiplexing gain.

4) *BLAST as a Subclass of GSTSK*: We may also view the BLAST architecture of Section I-B as a certain form of our GSTSK scheme of Fig. 6, by setting $P = Q = M$, $T = 1$ and using Eq. (8), where we have the relationship of

$$\mathbf{S}(i) = \frac{1}{\sqrt{M}} \begin{bmatrix} s_1 \\ \vdots \\ s_M \end{bmatrix} = s_1 \underbrace{\begin{bmatrix} \frac{1}{\sqrt{M}} \\ 0 \\ \vdots \\ 0 \end{bmatrix}}_{\mathbf{A}_1} + \dots + s_M \underbrace{\begin{bmatrix} 0 \\ \vdots \\ 0 \\ \frac{1}{\sqrt{M}} \end{bmatrix}}_{\mathbf{A}_M}.$$

This BLAST arrangement does not provide any explicit transmit diversity gain, and this property is shared by the SM/SSK schemes. Since the resultant system suffers from Inter-Antenna Interference (IAI) imposed on the AEs, the computational complexity of mitigating it becomes inevitably high, which increases with the number of AEs M .

5) *Coherent Space-Time Shift Keying*: Furthermore, in this contribution we refer to the special case of our GSTSK scheme, employing $P = 1$, as STSK proposed in Section II-B, where only one out of Q dispersion matrices is activated, which results in lower B_1 and B_2 values in comparison to our GSTSK scheme for the case of $P > 1$. This STSK arrangement enables us to implement single-stream-based

$$\begin{aligned}
\mathbf{S}(i) &= \frac{2}{3} \begin{bmatrix} s_1 & -s_2^* & -s_3^* & 0 \\ s_2 & s_1^* & 0 & -s_3^* \\ s_3 & 0 & s_1^* & s_2^* \end{bmatrix} \\
&= \underbrace{\begin{bmatrix} \frac{\sqrt{2}}{3} & 0 & 0 & 0 \\ 0 & \frac{\sqrt{2}}{3} & 0 & 0 \\ 0 & 0 & \frac{\sqrt{2}}{3} & 0 \end{bmatrix}}_{\mathbf{A}_1} \sqrt{2}\alpha_1 + j \underbrace{\begin{bmatrix} \frac{\sqrt{2}}{3} & 0 & 0 & 0 \\ 0 & -\frac{\sqrt{2}}{3} & 0 & 0 \\ 0 & 0 & -\frac{\sqrt{2}}{3} & 0 \end{bmatrix}}_{\mathbf{A}_2} \sqrt{2}\beta_1 + \underbrace{\begin{bmatrix} 0 & -\frac{\sqrt{2}}{3} & 0 & 0 \\ \frac{\sqrt{2}}{3} & 0 & 0 & 0 \\ 0 & 0 & 0 & \frac{\sqrt{2}}{3} \end{bmatrix}}_{\mathbf{A}_3} \sqrt{2}\alpha_2 \\
&+ j \underbrace{\begin{bmatrix} 0 & \frac{\sqrt{2}}{3} & 0 & 0 \\ \frac{\sqrt{2}}{3} & 0 & 0 & 0 \\ 0 & 0 & 0 & -\frac{\sqrt{2}}{3} \end{bmatrix}}_{\mathbf{A}_4} \sqrt{2}\beta_2 + \underbrace{\begin{bmatrix} 0 & 0 & -\frac{\sqrt{2}}{3} & 0 \\ 0 & 0 & 0 & -\frac{\sqrt{2}}{3} \\ \frac{\sqrt{2}}{3} & 0 & 0 & 0 \end{bmatrix}}_{\mathbf{A}_5} \sqrt{2}\alpha_3 + j \underbrace{\begin{bmatrix} 0 & 0 & \frac{\sqrt{2}}{3} & 0 \\ 0 & 0 & 0 & \frac{\sqrt{2}}{3} \\ \frac{\sqrt{2}}{3} & 0 & 0 & 0 \end{bmatrix}}_{\mathbf{A}_6} \sqrt{2}\beta_3 \quad (9)
\end{aligned}$$

low-complexity ML detection, similarly to SM/SSK. Furthermore, an appropriately-constructed set of dispersion matrices $\mathbf{A}_{q'}$ ($q' = 1, \dots, Q$) enables us to dispense with symbol-level IAS. More specifically, the structure of each dispersion matrix $\mathbf{A}_{q'}$ is constructed so that there is a single non-zero element for each column of the dispersion matrix $\mathbf{A}_{q'}$. This constraint enables us to avoid any simultaneous transmission by multiple antennas, also similarly to SM/SSK.

C. Optimal Hard-Decision ML Detector

Similarly to the optimal ML detector derived for the STSK scheme in Section II-D, we arrive at the linearized receiver's system model. It is worth mentioning that the GSTSK scheme's ML receiver is imposed by P ICI. Accordingly, the ML detection criterion is formulated as $(\hat{B}_1, \hat{B}_2) = \arg \min_{(B_1, B_2)} \|\bar{\mathbf{Y}} - \bar{\mathbf{H}}\chi\mathbf{K}\|^2$
 $= \arg \min_{(B_1, B_2)} \left\| \bar{\mathbf{Y}} - \sum_{q=1}^Q k_q \{\bar{\mathbf{H}}\chi\}_q \right\|^2$, where $\{\bar{\mathbf{H}}\chi\}_q$ denotes the q th column of $\bar{\mathbf{H}}\chi$. Note that the computational complexity imposed by calculating $\sum_{q=1}^Q k_q \{\bar{\mathbf{H}}\chi\}_q$ linearly increases with the parameter P , because the number of non-zero elements in k_q ($q = 1, \dots, Q$) is P as mentioned above.

More specifically, the computational complexity per bit for this detection scheme is evaluated in terms of the number of real-valued multiplications, which may be shown to be $4MNT^2Q + (4NTP + 2NT)f(Q, P)\mathcal{L}^P/B$. Here, we can find that the value P is in the exponent of \mathcal{L}^P . Fig. 7 shows the relationship between the complexity and the throughput of our QPSK-modulated GSTSK(2, 2, 2, 4, P) scheme designed for achieving the maximum diversity order of four, where the parameter P was varied from $P = 1$ to $P = 4$. As mentioned in Sections III-B2 and III-B5, our GSTSK schemes employing $P = 1$ and $P = Q$ correspond to the LDC and STSK schemes, respectively. As seen in Fig. 7, the normalized throughput R tends to increase with the value of P at the cost of an increased computational complexity, which explicitly show the rate-complexity tradeoff of our GSTSK scheme.

D. Unified DCMC Capacity

In this section we characterize the DCMC capacity [37] of our GSTSK framework. As mentioned above, members of

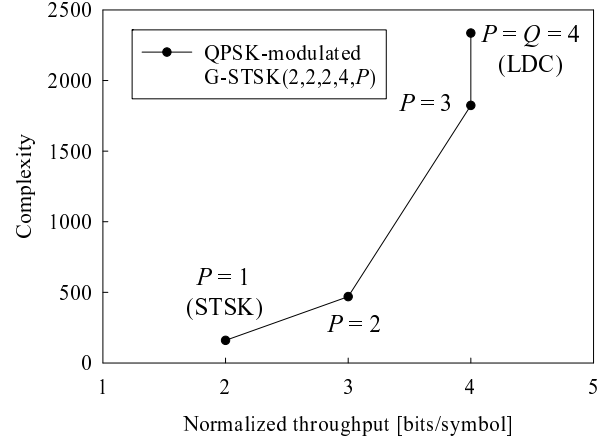


Fig. 7. The relationship between complexity and throughput of our QPSK-modulated GSTSK(2, 2, 2, 4, P) scheme of Fig. 6, achieving the maximum diversity order of four, where the parameter P was changed from $P = 1$ to $P = 4$.

the GSTSK family support many other MIMO arrangements, hence the resultant capacity equation is also applicable to diverse MIMOs.

According to [37], the DCMC capacity of our GSTSK scheme using \mathcal{L} -PSK/QAM signaling may be derived from that of the discrete memoryless channel as Eq. (10), which is at the top of this page. Under the assumption that all the signals $\mathbf{K}_{\beta_1, \beta_2}$ are equi-probable, i.e. when we have $P(\mathbf{K}_{1,1}) = \dots = P(\mathbf{K}_{2^{B_1}, 2^{B_2}}) = 1/2^B$, the DCMC capacity of our GSTSK scheme using \mathcal{L} -PSK/QAM signaling may be derived from that of the discrete memoryless channel as $C = \frac{1}{T} \left(B - \frac{1}{2^B} \sum_{\beta_1, \beta_2} E \left[\log_2 \left\{ \sum_{\beta'_1, \beta'_2} \exp(\Psi_{\beta_1, \beta_2}^{\beta'_1, \beta'_2}) \mathbf{K}_{\beta'_1, \beta'_2} \right\} \right] \right)$, where we have $\Psi_{\beta_1, \beta_2}^{\beta'_1, \beta'_2} = -\|\bar{\mathbf{H}}\chi(\mathbf{K}_{\beta_1, \beta_2} - \mathbf{K}_{\beta'_1, \beta'_2}) + \bar{\mathbf{V}}\|^2 + \|\bar{\mathbf{V}}\|^2$.

According to the unified capacity metric derived above, we plotted in Fig. 8 the DCMC capacity curves associated with the three different MIMO arrangements, i.e. the BLAST, the SM and the CSTSK schemes, each exhibiting the normalized transmission rate of $R = 3.0$ bits/symbol. We assumed that the CSTSK and the BLAST schemes employed $(M, N) = (3, 2)$ AEs, while the SM scheme had $(M, N) = (4, 2)$ AEs. As seen

$$C = \frac{1}{T} \max_{P(\mathbf{K}_{1,1}), \dots, P(\mathbf{K}_{2^{B_1}, 2^{B_2}})} \sum_{\beta_1, \beta_2} \int_{-\infty}^{\infty} \dots \int_{-\infty}^{\infty} P(\bar{\mathbf{Y}} | \mathbf{K}_{\beta_1, \beta_2}) \cdot P(\mathbf{K}_{\beta_1, \beta_2}) \log_2 \left[\frac{P(\bar{\mathbf{Y}} | \mathbf{K}_{\beta_1, \beta_2})}{\sum_{\beta'_1, \beta'_2} P(\bar{\mathbf{Y}} | \mathbf{K}_{\beta'_1, \beta'_2}) P(\mathbf{K}_{\beta'_1, \beta'_2})} \right] d\bar{\mathbf{Y}} \quad (\text{bits/symbol}). \quad (10)$$

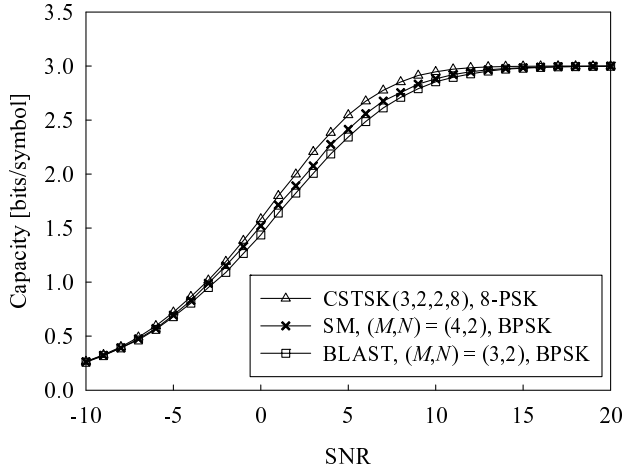


Fig. 8. DCMC capacity of the 8-PSK modulated CSTSK(3, 2, 2, 8) of Fig. 4, the BPSK-modulated SM scheme [61] of Fig. 3 having $(M, N)=(4, 2)$ antennas and the BPSK-modulated BLAST scheme having $(M, N)=(3, 2)$ antennas.

in Fig. 8, upon increasing the SNR value, each capacity curve converged to the attainable normalized throughput $R = 3.0$ bits/symbol. Accordingly, it was demonstrated that the DCMC capacity derived serves as a unified capacity limit of the diverse MIMO arrangements considered.

E. Achievable Diversity Order of Our GSTSK Scheme

In this section we introduce the achievable diversity order of our GSTSK scheme, based on the unconditional PEP of $P(\mathbf{S} \rightarrow \mathbf{S}')$, where the transmitted space-time matrix \mathbf{S} is misinterpreted as \mathbf{S}' . According to [18], the well-known PEP bound of general block-based STCs is represented by $P(\mathbf{S} \rightarrow \mathbf{S}') \leq \prod_{m=1}^M \left(1 + \frac{\mu_m}{4N_0}\right)^{-N}$, where μ_m is the m th eigenvalue of $(\mathbf{S} - \mathbf{S}')(\mathbf{S} - \mathbf{S}')^H$. Moreover, in the high-SNR regime, this Chernoff bound can be further approximated by

$$P(\mathbf{S} \rightarrow \mathbf{S}') \leq \underbrace{\frac{1}{2} \left(\frac{1}{4N_0}\right)^{m'N}}_{\text{diversity gain}} \cdot \underbrace{\prod_{m=1}^{m'} \frac{1}{\mu_m^N}}_{\text{coding gain}}, \quad (11)$$

where m' is the rank of $(\mathbf{S} - \mathbf{S}')(\mathbf{S} - \mathbf{S}')^H$. As seen from Eq. (11), the PEP can be divided into two components, namely the diversity gain and the coding gain.¹⁰ Furthermore, the

¹⁰To elaborate a little further, as shown in Chapter 5.2 of [39], while the diversity gain manifests itself in increasing the slope of the BER curve, the coding gain attained results in shifting the BER curve to a lower SNR region. This implies that the SNR advantage of a higher diversity gain is increased in the higher SNR region. By contrast, the coding gain typically remains constant at high SNRs.

achievable diversity order, which is typically defined as the slope of the PEP, is given by $m' \cdot N \leq \min(M, T) \cdot N$. This also indicates that the reduction in T may give rise to the reduction of the computational complexity, while increasing the normalized throughput at the cost of a reduced diversity gain.

F. Performance Results

In this contribution, we generated an appropriate dispersion-matrix set capable of achieving a good BER performance for each GSTSK arrangement, which were designed based on the well-known rank- and determinant-criterion [50] for the sake of simplicity, although we may readily employ other design criteria, such as the BLock Error Ratio BLER minimization technique of [73] and the DCMC-capacity maximization technique of [50]. Here, we assumed independently, identically distributed block Rayleigh fading scenarios, where each channel tap remains constant over a single space-time block duration. For simplicity, the effects of neither time- nor spatial-correlation were considered.

In Figs. 9 and 10 we compared the diverse GSTSK arrangements of Fig. 6 to other MIMOs, such as the CSTSK scheme of Fig. 4, the SM/SSK scheme of Fig. 3, the orthogonal STBC scheme and the BLAST scheme. More specifically, the system parameters employed in our simulations are listed in Table VI. In Fig. 9, $(M, N) = (3, 2)$ AEs were employed, where the transmission rates were given by $R = 3.0$ bits/symbol, while only the SM scheme employed $(M, N) = (4, 2)$ AEs. Also, in Fig. 10 we assumed having $(M, N) = (4, 3)$ AEs and the transmission rates were given by $R = 4.0$ bits/symbol. Observe in Figs. 9 and 10 that our GSTSK scheme tended to outperform the CSTSK scheme, which was the explicit benefit of its more flexible system design. However, the GSTSK's performance advantage over the CSTSK scheme was at the expense of imposing on increased computational complexity invested in mitigating the effects of the P ICI contributions. Furthermore, it was also confirmed in Figs. 9 and 10 that our GSTSK scheme had a better BER performance, than conventional MIMO arrangements, such as the SM/SSK, the OSTBC and the BLAST schemes. We also note that although the OSTBC schemes achieved the maximum achievable diversity order of $M \cdot N$, the corresponding BER curves of Figs. 9 and 10 were inferior in comparison to the GSTSK and the CSTSK schemes. This is mainly due to the fact that the OSTBC schemes had to employ a high modulation order, such as 64- and 256-QAM, in order to attain transmission rates that were comparable to those of the BLAST, GSTSK and CSTSK schemes.

Also, observe in Fig. 9 that the BER curve of the CSTSK scheme was slightly better than that of the ACSTSK scheme,

TABLE VI
SYSTEM PARAMETERS OF THE UNCODED GSTSK SCHEME OF FIG. 6

Number of transmit antennas	M
Number of receive antennas	N
Symbol durations per block	T
Number of dispersion matrices	Q
Number of activated dispersion matrices	P
Modulation	\mathcal{L} -PSK or \mathcal{L} -QAM
Channels	Frequency-flat Rayleigh fading
Channel's coherence-time	$\tau = 1$ block duration
Detector	ML detector

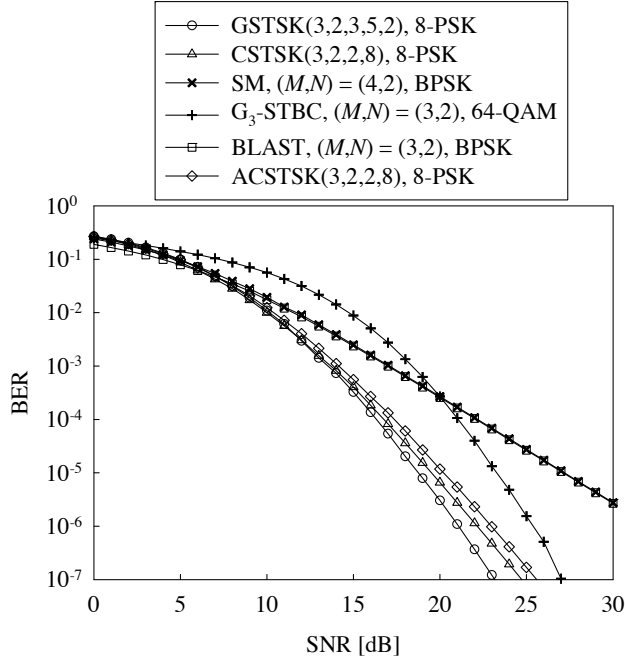


Fig. 9. BER comparison of our uncoded 8-PSK modulated GSTSK(3, 2, 3, 5, 2), the 8-PSK modulated CSTSK(3, 2, 2, 8) / ACSTSK(3, 2, 2, 8), the BPSK-modulated SM [61], the 64-QAM assisted G_3 -STBC [14] and the BPSK-modulated BLAST schemes.

albeit both exhibited a similar diversity order. As mentioned in Section II-C, this is mainly due to the fact that ACSTSK scheme's limited set of dispersion matrices limited the achievable performance, especially for a high Q value.¹¹

G. Design Guidelines

In order to design the GSTSK architecture, the related six parameters, namely $(\mathcal{L}, M, N, T, Q, P)$ as well as the Q dispersion matrices \mathbf{A}_q ($q = 1, \dots, Q$) have to be determined according to the following steps.

- The values of (M, N) represent the number of transmit and receive AEs.

¹¹To provide further insights, there is also a rate-diversity tradeoff between the ACSTSK and the SM schemes, both dispensing with perfect inter-antenna synchronization. For example, QPSK-modulated ACSTSK(3, N , 3, 4) theoretically achieves the normalized throughput of $R = \log_2(4 \cdot 4)/3 = 1.33$ bits/symbol as well as the maximum attainable diversity order of $\mathcal{O} = 3N$, while the corresponding parameters of the QPSK-modulated SM scheme having $(M, N) = (3, N)$ AEs [66] are $R = \log_2(3 \cdot 4) = 3.59$ bits/symbol and $\mathcal{O} = N$.

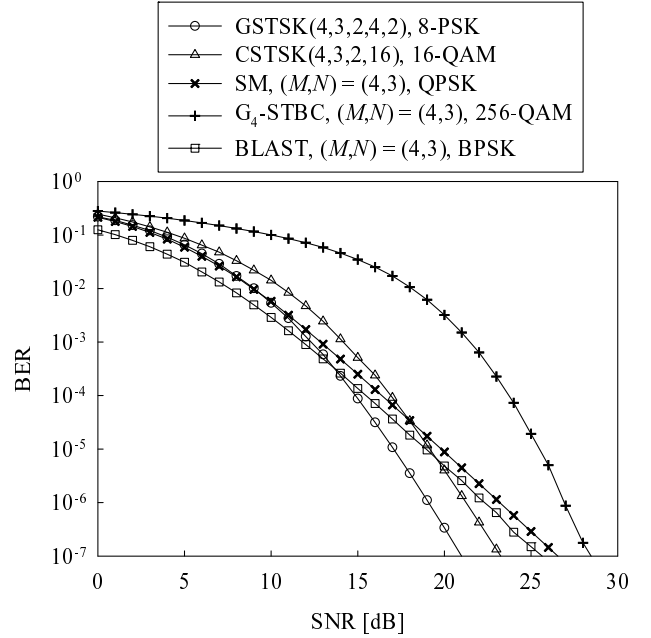


Fig. 10. BER comparison of our uncoded 8-PSK modulated GSTSK(4, 3, 2, 4, 2), the 16-QAM modulated CSTSK(4, 3, 2, 16), the QPSK-modulated SM [61], the 256-QAM assisted G_4 -STBC [14] and the BPSK-modulated BLAST schemes.

- The values of (\mathcal{L}, T, Q, P) are chosen so as to satisfy the desirable rate-, diversity- and complexity-tradeoffs characterized by the rate of $R = \frac{\log_2 f(Q, P) + P \log_2 \mathcal{L}}{T}$, the maximum attainable diversity order of $N \cdot \min(M, T)$ and the computational complexity of $[4MNT^2Q + (4NTP + 2NT)f(Q, P)\mathcal{L}^P/B]$.
- The Q dispersion matrices \mathbf{A}_q ($q = 1, \dots, Q$) are designed based on the DCMC-capacity maximization criterion or the rank- and determinant-criterion.

Since in practice we may have several potential options for $(\mathcal{L}, M, N, T, Q, P)$, their performance comparison is required in order to choose the most appropriate set.

IV. FURTHER STSK-RELATED STUDIES

In addition to the above-mentioned STSK family, such as the CSTSK, the ACSTSK and the GSTSK schemes, further related classes have been developed, which will be described below.

A. Non-Coherent Space-Time Shift Keying

In this context, we proposed the novel STSK concept, which facilitates a flexible and efficient MIMO implementation, while subsuming diverse classic MIMO arrangements. In reality, when the channel changes slowly in comparison to the symbol duration employed, the receiver can accurately estimate the CSI, based on the pilot symbols inserted in the transmitted signals. On the other hand, it is a challenging task to acquire accurate CSI for each MIMO-link for high-speed vehicles, which may require a high pilot overhead and imposes a substantial complexity. Furthermore, the resultant CSI estimation error is expected to erode the achievable performance, as shown in Chapter 8 of [50]. Hence, it is beneficial to employ a MIMO arrangements, which do not require channel estimates either at the transmitter or at the receiver.

To this end, in [56], [57] the Differentially-encoded STSK (DSTSK) scheme was also proposed, which retains the fundamental benefits of the coherent STSK scheme, although naturally, the corresponding non-coherent receiver suffers from the usual performance loss compared to its coherent counterpart. To be more specific, inspired by the coherent STSK scheme of Section II-B, the new concept of DSTSK is proposed as a unified differential MIMO scheme, which is capable of striking a flexible diversity-versus-multiplexing gains tradeoff. Similarly to coherent STSK, we have an ICI-free system model, hence our DSTSK receiver is capable of using low-complexity the single-stream-based optimal ML detection in uncoded scenarios.

In order to further improve the DSTSK scheme's performance as well as to combat the effects of the Doppler Shift, a Multiple-Symbol Differential Sphere Detector (MSDSD)-assisted non-coherent detection algorithm was developed for the DSTSK in [74]. This technique mitigates the potential performance degradation of noncoherent receivers encountered in rapidly fading channels, while circumventing the exponentially increasing complexity of MSDD.

Moreover, in [75] a semi-blind joint channel estimation and data detection scheme was applied to the STSK arrangement, resulting in a beneficial coherent detection aided algorithm. More specifically, in this scheme the low-complexity least square channel estimation and the single-stream-based ML detection are iteratively carried out, with the aid of the minimum number of training blocks. This technique substantially reduces the pilot-overhead, while approaching the optimal ML performance at high SNRs.

B. Distributed Space-Time Shift Keying

As mentioned above, we have highlighted a range of novel MIMO concepts, which included coherent STSK, differential STSK and generalized STSK schemes. To be specific, we mainly focused our attention on co-located MIMO scenarios, where multiple antennas were accommodated at the transmitter and/or at the receiver, which may however suffer from the effects of inter-antenna correlation imposed by insufficient antenna separation. To this end, the recent philosophy of cooperative communication [76]–[93] may be considered to be a promising approach, where the concept of Virtual Antenna

Arrays (VAAs) enables us to exploit additional degrees of design freedom. More specifically, it is often claimed that cooperative MIMO systems are capable of attaining the maximum achievable diversity gain associated with uncorrelated fading. However, most of the previous studies related to cooperative MIMOs typically employed idealized assumptions, which are difficult to satisfy in practice.

More recently, a practical cooperative MIMO arrangement based on the above-mentioned STSK philosophy was proposed in [94], [95], which enables us to adapt the number of Relay Nodes (RNs), the transmission rate as well as the achievable diversity order, depending on the associated system requirements and channel conditions, owing to its design flexibility. In this scheme, considering the usual twin-phase cooperative transmission regime constituted by a broadcast phase and by a cooperative phase, the CSTSK and DSTSK schemes developed for co-located MIMO systems are employed during the cooperative transmission phase. At the Destination Node (DN), the received signals of the direct Source-Destination (SD) link and of the Relay-Destination (RD) links are jointly detected using ICI-free low-complexity single-stream ML detection. Furthermore, it was also demonstrated in [94], [95] that our cooperative STSK arrangement is capable of outperforming its cooperative OSTBC counterparts.

V. CONCLUSIONS

A. Summary of the Paper

In this tutorial, after reviewing the diverse MIMO arrangements, then we have provided detailed MIMO transceiver designs employing the novel STSK encoding concept for enhancing their achievable performance. More specifically, we firstly presented the theory and fundamental design of the coherent STSK scheme, which activates one out of Q dispersion matrices during each transmitted block and allows us to strike a flexible diversity versus rate tradeoff. We demonstrated that our CSTSK scheme is capable of utilizing a realistic single-stream-based ML detector due to the absence of any ICI. Additionally, we proposed a modified version of the STSK scheme, namely the ACSTSK scheme, which dispenses with the requirement of perfect IAS. Moreover, we further generalized the CSTSK scheme for the sake of striking flexible tradeoffs between the throughput, the diversity gain and the computational complexity. This is achieved by GSTSK concept, which simultaneously activates P out of Q dispersion matrices during each block interval. Also, we assured that our GSTSK scheme subsumes diverse MIMO schemes, such as the OSTBCs, the BLAST scheme, the LDCs, the SM/SSK scheme and the CSTSK scheme. Furthermore, the design guidelines of our CSTSK and GSTSK schemes were provided as Algorithms 1 and 2, respectively.

Finally, we discussed other classes of STSK, exhibiting different functions, which are differentially-encoded STSK scheme, cooperative STSK scheme and serially-concatenated three-stage turbo-coded STSK scheme.

B. Future Research Ideas

In this paper, we considered only a random search method for dispersion-matrix optimization, for the sake of simplicity.

More specifically, the rank- and determinant-criterion was used for the cost function of CSTSK and GSTSK schemes. However, there are numerous other approaches, which may potentially simplify the dispersion-matrix optimization, while achieving a higher performance. For example, it might be useful to optimize the dispersion matrices with the aid of Genetic Algorithms (GAs), as proposed in [96] in the context of the LDCs.

Furthermore, in this paper we proposed the GSTSK scheme, which simultaneously activates P out of Q dispersion matrices. In this scheme, upon increasing the value of P , the GSTSK receiver has to cope with the equivalent number of ICI contributions. Thus, a higher P leads to a higher computational complexity at the receiver, although it enhances the bandwidth efficiency. We introduced the optimal ML detector for the uncoded scenario, which may result in a high complexity for a high- P scenario. To this end, it may be useful to develop more efficient near-optimal detectors for the GSTSK scheme, such as the Sphere Detector (SD) [97], the GA-aided detector [98], the Markov Chain Monte Carlo (MCMC) detector [99]–[101], the Ant-Colony Optimization (ACO) detector [102] and the Particle Swarm Optimization (PSO) detector [103].

VI. GLOSSARY

ACO	Ant-Colony Optimization
ACSTSK	Asynchronous Coherent Space-Time Shift Keying
AEs	Antenna Elements
AWGN	Additive White Gaussian Noise
BER	Bit-Error Ratio
BLAST	Bell Labs Layered Space-Time
BPSK	Binary Phase-Shift Keying
BS	Base Station
CDD	Cyclic Delay Diversity
CIRs	Channel Impulse Responses
CSI	Channel State Information
CSTSK	Coherent Space-Time Shift Keying
DCMC	Discrete-input Continuous-output Memoryless Channel
DL	Down-Link
DOAs	Directions-of-Arrival
DODs	Directions-of-Departure
DSTCs	Differential Space-Time Codes
DSTSK	Differentially-encoded Space-Time Shift Keying
EGC	Equal Gain Combining
GA	Genetic Algorithm
GSTSK	Generalized Space-Time Shift Keying
IAI	Inter-Antenna Interference
IAS	Inter-Antenna Synchronization
ICI	Inter-Channel Interference
LDC	Linear Dispersion Code
MAP	Maximum A Priori
MCMC	Markov Chain Monte Carlo
MIMO	Multiple-Input Multiple-Output
ML	Maximum Likelihood
MMSE	Minimum Mean-Square Error
MRC	Maximum-Ratio Combining
MSDD	Multiple-Symbol Differential Detection
MSDSD	Multiple-Symbol Differential Sphere Detector
MU-MIMO	Multi-User Multiple-Input Multiple-Output
MUD	Multi-User Detection
MUT	Multi-User Transmission
OFDM	Orthogonal Frequency-Division Multiplexing
OSTBCs	Orthogonal Space-Time Block Codes
PSK	Phase-Shift Keying
PSO	Particle Swarm Optimization
QAM	Quadrature Amplitude Modulation
QPSK	Quadrature Phase-Shift Keying
QOSTBCs	Quasi-Orthogonal Space-Time Block Codes
RD	Relay-Destination
RN	Relay Node
SC	Selection Combining
SD	Sphere Detection
SDM	Space Division Multiplexing
SDMA	Space Division Multiple Access
SISO	Soft-Input Soft-Output
SM	Spatial Modulation
SNR	Signal-to-Noise Ratio
SR	Source-Relay
SSK	Space-Shift Keying
ST	Space-Time
STBCs	Space-Time Block Codes
STCs	Space-Time Codes
STS	Space-Time Spreading
STSK	Space-Time Shift Keying
STTCs	Space-Time Trellis Codes
TASTBCs	Threaded Algebraic Space-Time Block Codes
TVLT	Time Variant Linear Transformation
USTM	Unitary Space-Time Modulation
UWB	Ultra-Wide Bandwidth
VAA	Virtual Antenna Array

$$\mathbf{A}_1 = \begin{bmatrix} 0.3313 - j0.0934 & -0.2093 + j0.0059 & 0.3430 - j0.1426 \\ 0.0256 - j0.2123 & 0.4258 - j0.1198 & -0.1492 + j0.3136 \\ -0.2001 - j0.1485 & -0.4746 - j0.7163 & 0.1930 + j0.0034 \end{bmatrix}, \quad (12)$$

$$\mathbf{A}_2 = \begin{bmatrix} 0.0533 - j0.5840 & -0.2676 + j0.0331 & 0.2379 + j0.2635 \\ -0.3727 + j0.1888 & -0.2517 - j0.3823 & 0.1967 + j0.1229 \\ -0.2409 - j0.0039 & 0.0660 - j0.0738 & -0.6645 + j0.1008 \end{bmatrix}, \quad (13)$$

$$\mathbf{A}_3 = \begin{bmatrix} -0.4773 + j0.0533 & -0.1435 + j0.2393 & 0.5933 - j0.0776 \\ 0.2637 + j0.0093 & -0.2280 - j0.4797 & 0.1906 + j0.0211 \\ 0.2209 - j0.2538 & -0.0108 - j0.2367 & 0.5170 - j0.0911 \end{bmatrix}, \quad (14)$$

$$\mathbf{A}_4 = \begin{bmatrix} 0.1434 + j0.2098 & -0.3781 - j0.1050 & -0.5476 + j0.0826 \\ -0.0158 + j0.2100 & 0.1294 - j0.5712 & -0.3051 + j0.0995 \\ -0.1745 + j0.5746 & -0.1668 - j0.1640 & 0.0265 - j0.2613 \end{bmatrix}, \quad (15)$$

$$\mathbf{A}_5 = \begin{bmatrix} 0.1083 + j0.1886 & -0.3862 + j0.4963 & -0.3009 + j0.0908 \\ 0.3435 - j0.4493 & -0.1621 + j0.0307 & 0.0856 + j0.0560 \\ 0.0548 - j0.4980 & -0.2469 + j0.3589 & -0.3752 - j0.1402 \end{bmatrix}. \quad (16)$$

APPENDIX DISPERSION-MATRIX SET EMPLOYED FOR THE SIMULATIONS

Parts of the dispersion-matrix sets $\mathbf{A}_{q'}$ ($q' = 1, \dots, Q$), which were used for our simulations in Fig. 9 are as follows. While the dispersion-matrix set of the 8-PSK modulated GSTSK(3, 2, 3, 5, 2) scheme is given by Eqs. (12)–(16), those of the 8-PSK modulated CSTSK(3, 2, 2, 8) and ACSTSK(3, 2, 2, 8) schemes correspond to Eqs. (17)–(24) and Eqs. (25)–(32), respectively.¹²

• 8-PSK modulated CSTSK(3, 2, 2, 8) scheme

$$\mathbf{A}_1 = \begin{bmatrix} -0.3004 - j0.0851 & -0.5751 + j0.1096 \\ -0.1276 + j1.0183 & -0.2113 + j0.1873 \\ -0.3897 + j0.1733 & -0.3467 - j0.3532 \end{bmatrix}, \quad (17)$$

$$\mathbf{A}_2 = \begin{bmatrix} 0.0417 - j0.1950 & 0.6609 + j0.3697 \\ -0.3282 + j0.6485 & 0.7036 - j0.1895 \\ 0.3958 + j0.3428 & -0.1143 - j0.2006 \end{bmatrix}, \quad (18)$$

$$\mathbf{A}_3 = \begin{bmatrix} 0.6896 - j0.2101 & 0.2777 + j0.3861 \\ 0.1139 + j0.1366 & 0.3816 - j0.0568 \\ -0.1513 + j0.3383 & 0.5344 + j0.8067 \end{bmatrix}, \quad (19)$$

$$\mathbf{A}_4 = \begin{bmatrix} -0.4194 + j0.3000 & -0.1861 + j0.0637 \\ -0.4607 + j0.3887 & 0.2187 + j0.6741 \\ -0.0900 - j0.2984 & 0.1206 + j0.8475 \end{bmatrix}, \quad (20)$$

$$\mathbf{A}_5 = \begin{bmatrix} -0.3674 - j0.0757 & -0.1060 + j0.4035 \\ 0.0179 - j0.3796 & 0.2175 + j0.3668 \\ -0.8406 + j0.0350 & -0.1652 - j0.7899 \end{bmatrix}. \quad (21)$$

$$\mathbf{A}_6 = \begin{bmatrix} -0.3842 - j0.4024 & 0.3809 - j0.2354 \\ -0.3558 - j0.3678 & 0.2873 - j0.6271 \\ -0.2225 + j0.4551 & 0.4703 + j0.5240 \end{bmatrix}. \quad (22)$$

$$\mathbf{A}_7 = \begin{bmatrix} -0.1888 - j0.5969 & -0.5091 - j0.2274 \\ 0.3276 + j0.0346 & -0.3845 + j0.5597 \\ -0.1933 + j0.2262 & 0.3727 - j0.7072 \end{bmatrix}. \quad (23)$$

$$\mathbf{A}_8 = \begin{bmatrix} 0.4781 - j0.5985 & -0.3340 - j0.2010 \\ -0.4031 - j0.1665 & 0.5244 + j0.1485 \\ 0.4878 + j0.4562 & 0.5505 + j0.1582 \end{bmatrix}. \quad (24)$$

• 8-PSK modulated ACSTSK(3, 2, 2, 8) scheme

$$\mathbf{A}_1 = \begin{bmatrix} 0.0000 + j0.0000 & 0.8436 - j0.9298 \\ -0.2706 + j0.5921 & 0.0000 + j0.0000 \\ 0.0000 + j0.0000 & 0.0000 + j0.0000 \end{bmatrix}, \quad (25)$$

$$\mathbf{A}_2 = \begin{bmatrix} -0.6411 + j1.0414 & 0.0000 + j0.0000 \\ 0.0000 + j0.0000 & 0.0000 + j0.0000 \\ 0.0000 + j0.0000 & 0.3679 + j0.6075 \end{bmatrix}, \quad (26)$$

$$\mathbf{A}_3 = \begin{bmatrix} 0.0000 + j0.0000 & 0.0000 + j0.0000 \\ 0.0000 + j0.0000 & 0.9449 - j0.5379 \\ 0.2080 + j0.8801 & 0.0000 + j0.0000 \end{bmatrix}, \quad (27)$$

$$\mathbf{A}_4 = \begin{bmatrix} 0.0000 + j0.0000 & 0.0000 + j0.0000 \\ 0.8484 - j0.7805 & 0.0000 + j0.0000 \\ 0.0000 + j0.0000 & 0.6098 + j0.5468 \end{bmatrix}, \quad (28)$$

$$\mathbf{A}_5 = \begin{bmatrix} 0.7376 - j0.5365 & 0.0000 + j0.0000 \\ 0.0000 + j0.0000 & 0.0000 + j0.0000 \\ 0.0000 + j0.0000 & -0.9906 + j0.4320 \end{bmatrix}. \quad (29)$$

$$\mathbf{A}_6 = \begin{bmatrix} 0.0000 + j0.0000 & 0.0000 + j0.0000 \\ -0.4834 + j0.6672 & 0.0000 + j0.0000 \\ 0.0000 + j0.0000 & -0.8728 + j0.7480 \end{bmatrix}. \quad (30)$$

$$\mathbf{A}_7 = \begin{bmatrix} 0.0000 + j0.0000 & -0.4865 - j0.7053 \\ 0.5867 - j0.9601 & 0.0000 + j0.0000 \\ 0.0000 + j0.0000 & 0.0000 + j0.0000 \end{bmatrix}. \quad (31)$$

$$\mathbf{A}_8 = \begin{bmatrix} 0.0000 + j0.0000 & 0.0000 + j0.0000 \\ 0.0000 + j0.0000 & 0.5145 - j0.0585 \\ 1.0281 + j0.8215 & 0.0000 + j0.0000 \end{bmatrix}. \quad (32)$$

REFERENCES

- [1] G. J. Foschini, "Layered space-time architecture for wireless communication in a fading environment when using multi-element antennas," *Bell Labs Technical Journal*, vol. 1, no. 2, pp. 41–59, 1996.
- [2] G. J. Foschini and M. J. Gans, "On limits of wireless communications in a fading environment when using multiple antennas," *Wireless Personal Communications*, vol. 6, no. 3, pp. 311–335, 1998.
- [3] I. E. Telatar, "Capacity of multi-antenna Gaussian channels," *European transactions on telecommunications*, vol. 10, no. 6, pp. 585–595, 1999.
- [4] S. M. Alamouti, "A simple transmit diversity technique for wireless communications," *IEEE J. Sel. Areas Commun.*, vol. 16, no. 8, pp. 1451–1458, 1998.
- [5] V. Tarokh, H. Jafarkhani, and A. R. Calderbank, "Space-time block codes from orthogonal designs," *IEEE Trans. Inf. Theory*, vol. 45, no. 5, pp. 1456–1467, 1999.
- [6] V. Tarokh, N. Seshadri, and A. R. Calderbank, "Space-time codes for high data rate wireless communication: performance criterion and code construction," *IEEE Trans. Inf. Theory*, vol. 44, no. 2, pp. 744–765, 1998.
- [7] L. Hanzo, T. H. Liew, and B. L. Yeap, *Turbo Coding, Turbo Equalisation, and Space-Time Coding for Transmission over Fading Channels*. John Wiley and IEEE Press, 2002.

¹²Here, in order to optimize the sets of dispersion matrices used for our simulations, we employed the above-mentioned determinant-criterion, while maintaining full rank. To be more specific, for the CSTSK/GSTSK schemes, we randomly generated a sufficiently high number of ($M \times T$)-element dispersion-matrix sets under the power constraints [57], where each matrix element obeys the Gaussian distribution. Throughout our investigations, we found that 10^6 – 10^8 random dispersion-matrix generations were typically required in order to achieve a good BER, depending on the matrix-size employed.

- [8] A. Goldsmith, *Wireless communications*. Cambridge University Press, 2005.
- [9] B. Hassibi and B. M. Hochwald, "High-rate codes that are linear in space and time," *IEEE Trans. Inf. Theory*, vol. 48, no. 7, pp. 1804–1824, 2002.
- [10] D. G. Brennan, "Linear diversity combining techniques," *Proceedings of the IRE*, vol. 47, no. 6, pp. 1075–1102, 1959.
- [11] A. Goldsmith, "Capacity of Rayleigh fading channels under different adaptive transmission and diversity-combining techniques," *IEEE Trans. Veh. Technol.*, vol. 48, no. 4, pp. 1165–1181, 1999.
- [12] A. Wittneben, "Basestation modulation diversity for digital SIMULCAST," in *41st IEEE Vehicular Technology Conference*, St. Louis, MO, 1991, pp. 848–853.
- [13] N. Seshadri and J. H. Winters, "Two signaling schemes for improving the error performance of frequency-division-duplex (FDD) transmission systems using transmitter antenna diversity," in *43rd IEEE Vehicular Technology Conference*, Secaucus, NJ, 1993, pp. 508–511.
- [14] V. Tarokh, H. Jafarkhani, and A. R. Calderbank, "Space-time block coding for wireless communications: performance results," *IEEE J. Sel. Areas Commun.*, vol. 17, no. 3, pp. 451–460, 1999.
- [15] H. Jafarkhani, "A quasi-orthogonal space-time block code," *IEEE Trans. Commun.*, vol. 49, no. 1, pp. 1–4, 2001.
- [16] Y. Xin, Z. Wang, and G. B. Giannakis, "Space-time diversity systems based on linear constellation precoding," *IEEE Trans. Wireless Commun.*, vol. 2, no. 2, 2003.
- [17] H. E. Gamal and M. O. Damen, "Universal space-time coding," *IEEE Trans. Inf. Theory*, vol. 49, no. 5, pp. 1097–1119, 2003.
- [18] V. Tarokh, N. Seshadri, and A. R. Calderbank, "Space-time codes for high data rate wireless communication: Performance criterion and code construction," *IEEE Trans. Inf. Theory*, vol. 44, no. 2, pp. 744–765, 1998.
- [19] L. Hanzo, S. X. Ng, T. Keller, and W. Webb, *Quadrature Amplitude Modulation: From Basics to Adaptive Trellis-Coded, Turbo-Equalised and Space-Time Coded OFDM, CDMA and MC-CDMA Systems*. John Wiley and IEEE Press, 2004.
- [20] B. Hochwald, T. L. Marzetta, and G. B. Papadias, "A transmitter diversity scheme for wideband CDMA systems based on space-time spreading," *IEEE J. Sel. Areas Commun.*, vol. 19, no. 1, pp. 48–60, 2001.
- [21] A. Dammann and S. Kaiser, "Standard conformable antenna diversity techniques for OFDM and its application to the DVB-T system," in *IEEE Global Communications Conference (GLOBECOM)*, vol. 5, 2001, pp. 3100–3105.
- [22] A. Lodhi, F. Said, M. Dohler, and A. Aghvami, "Performance comparison of space-time block coded and cyclic delay diversity MC-CDMA systems," *IEEE Wireless Commun.*, vol. 12, no. 2, pp. 38–45, 2005.
- [23] V. Tarokh and H. Jafarkhani, "A differential detection scheme for transmit diversity," *IEEE J. Sel. Areas Commun.*, vol. 18, no. 7, pp. 1169–1174, 2000.
- [24] B. M. Hochwald and T. L. Marzetta, "Unitary space-time modulation for multiple-antenna communications in Rayleigh flat fading," *IEEE Trans. Inf. Theory*, vol. 46, no. 2, pp. 543–564, 2000.
- [25] B. L. Hughes, "Differential space-time modulation," *IEEE Trans. Inf. Theory*, vol. 46, no. 7, pp. 2567–2578, 2000.
- [26] Z. Liu, G. B. Giannakis, and B. L. Hughes, "Double differential space-time block coding for time-selective fading channels," *IEEE Trans. Commun.*, vol. 49, no. 9, pp. 1529–1539, 2001.
- [27] R. Schober and L. H. J. Lampe, "Noncoherent receivers for differential space-time modulation," *IEEE Trans. Commun.*, vol. 50, no. 5, pp. 768–777, 2002.
- [28] Y. Zhu and H. Jafarkhani, "Differential modulation based on quasi-orthogonal codes," *IEEE Trans. Wireless Commun.*, vol. 4, no. 6, pp. 3005–3017, 2005.
- [29] P. W. Wolniansky, G. J. Foschini, G. D. Golden, and R. A. Valenzuela, "V-BLAST: An architecture for realizing very high data rates over the rich-scattering wireless channel," in *Proc. International Symposium on Signals, Systems, and Electronics (ISSSE'98)*, Pisa, Italy, 1998, pp. 295–300.
- [30] S. Sugiura, S. Chen, and L. Hanzo, "MIMO-aided near-capacity turbo transceivers: Taxonomy and performance versus complexity," *IEEE Commun. Surveys Tutorials*, pp. 1–22, in press.
- [31] P. W. Golden, C. J. Foschini, R. Valenzuela, and P. W. Wolniansky, "Detection algorithm and initial laboratory results using V-BLAST space-time communication architecture," *Electronics Letters*, vol. 35, no. 1, pp. 14–16, 1999.
- [32] E. Viterbo and J. Boutros, "A universal lattice code decoder for fading channels," *IEEE Trans. Inf. Theory*, vol. 45, no. 5, pp. 1639–1642, 1999.
- [33] F. Hasegawa, J. Luo, K. R. Pattipati, P. Willett, and D. Pham, "Speed and accuracy comparison of techniques for multiuser detection in synchronous CDMA," *IEEE Trans. Commun.*, vol. 52, no. 4, pp. 540–545, 2004.
- [34] H. Sampath, P. Stoica, and A. Paulraj, "Generalized linear precoder and decoder design for MIMO channels using the weighted MMSE criterion," *IEEE Trans. Commun.*, vol. 49, no. 12, pp. 2198–2206, 2001.
- [35] G. J. Foschini and M. J. Gans, "On limits of wireless communications in a fading environment when using multiple antennas," *Wireless personal communications*, vol. 6, no. 3, pp. 311–335, 1998.
- [36] C. E. Shannon, "A mathematical theory of communication," *ACM SIGMOBILE Mobile Computing and Communications Review*, vol. 5, no. 1, pp. 3–55, 2001.
- [37] S. X. Ng and L. Hanzo, "On the MIMO channel capacity of multidimensional signal sets," *IEEE Trans. Veh. Technol.*, vol. 55, no. 2, pp. 528–536, 2006.
- [38] M. Jiang and L. Hanzo, "Multiuser MIMO-OFDM for next-generation wireless systems," *Proc. IEEE*, vol. 95, no. 7, pp. 1430–1469, 2007.
- [39] A. Paulraj, R. Nabar, and D. Gore, *Introduction to Space-Time Wireless Communications*. Cambridge University Press, 2003.
- [40] L. C. Godara, "Applications of antenna arrays to mobile communications I: Performance improvement, feasibility, and system considerations," *Proceedings of the IEEE*, vol. 85, no. 7, pp. 1031–1060, 1997.
- [41] —, "Application of antenna arrays to mobile communications II: Beam-forming and direction-of-arrival considerations," *Proc. IEEE*, vol. 85, no. 8, pp. 1195–1245, 1997.
- [42] L. Hanzo, J. Blough, and S. Ni, *3G, HSPA and FDD versus TDD Networking: Smart Antennas and Adaptive Modulation*. John Wiley and IEEE Press, 2008.
- [43] J. H. Winters, "Smart antennas for wireless systems," *IEEE Personal Commun.*, vol. 5, no. 1, pp. 23–27, 1998.
- [44] L. Zheng and D. N. C. Tse, "Diversity and multiplexing: a fundamental tradeoff in multiple-antenna channels," *IEEE Trans. Inf. Theory*, vol. 49, no. 5, pp. 1073–1096, 2003.
- [45] V. Tarokh, A. Naguib, N. Seshadri, and A. R. Calderbank, "Combined array processing and space-time coding," *IEEE Trans. Inf. Theory*, vol. 45, no. 4, pp. 1121–1128, 1999.
- [46] B. Hassibi and B. M. Hochwald, "Cayley differential unitary space-time codes," *IEEE Trans. Inf. Theory*, vol. 48, no. 6, pp. 1485–1503, 2002.
- [47] G. Jongren, M. Skoglund, and B. Ottersten, "Combining beamforming and orthogonal space-time block coding," *IEEE Trans. Inf. Theory*, vol. 48, no. 3, pp. 611–627, 2002.
- [48] M. Tao and R. S. Cheng, "Generalized layered space-time codes for high data rate wireless communications," *IEEE Trans. Wireless Commun.*, vol. 3, no. 4, pp. 1067–1075, 2004.
- [49] M. El-Hajjar, B. Hu, L.-L. Yang, and L. Hanzo, "Coherent and differential downlink space-time steering aided generalised multicarrier DS-CDMA," *IEEE Trans. Wireless Commun.*, vol. 6, no. 11, pp. 3857–3863, November 2007.
- [50] L. Hanzo, O. Alamri, M. El-Hajjar, and N. Wu, *Near-capacity Multi-functional MIMO Systems: Sphere-packing, Iterative Detection and Cooperation*. John Wiley and IEEE Press, 2009.
- [51] R. W. Heath and A. J. Paulraj, "Switching between diversity and multiplexing in MIMO systems," *IEEE Trans. Commun.*, vol. 53, no. 6, pp. 962–968, 2005.
- [52] H. E. Gamal, G. Caire, and M. O. Damen, "The MIMO ARQ channel: Diversity-multiplexing-delay tradeoff," *IEEE Trans. Inf. Theory*, vol. 52, no. 8, pp. 3601–3621, 2006.
- [53] M. El-Hajjar and L. Hanzo, "Layered steered space-time codes and their capacity," *Electronics Letters*, vol. 43, no. 12, pp. 680–682, 2007.
- [54] A. Sezgin, E. A. Jorswieck, and E. Costa, "LDC in MIMO Ricean channels: Optimal transmit strategy with MMSE detection," *IEEE Trans. Signal Process.*, vol. 56, no. 1, pp. 313–328, 2008.
- [55] N. Wu and L. Hanzo, "Near-capacity irregular-convolutional-coding-aided irregular precoded linear dispersion codes," *IEEE Trans. Veh. Technol.*, vol. 58, no. 6, pp. 2863–2871, 2009.
- [56] S. Sugiura, S. Chen, and L. Hanzo, "Space-time shift keying: A unified MIMO architecture," in *IEEE Global Communications Conference (GLOBECOM)*, Miami, Florida, USA, 6–10 December 2010.
- [57] —, "Coherent and differential space-time shift keying: A dispersion matrix approach," *IEEE Trans. Commun.*, vol. 58, no. 11, pp. 3219–3230, 2010.
- [58] R. W. Heath and A. J. Paulraj, "Linear dispersion codes for MIMO systems based on frame theory," *IEEE Trans. Signal Process.*, vol. 50, no. 10, pp. 2429–2441, 2002.

- [59] R. Mesleh, H. Haas, C. W. Ahn, and S. Yun, "Spatial modulation – a new low complexity spectral efficiency enhancing technique," in *First International Conference on Communications and Networking (CHINACOM)*, Beijing, China, Oct. 2006, pp. 1–5.
- [60] R. Mesleh, H. Haas, S. Sinanovic, C. W. Ahn, and S. Yun, "Spatial modulation," *IEEE Trans. Veh. Technol.*, vol. 57, no. 4, pp. 2228–2242, 2008.
- [61] J. Jeganathan, A. Ghayeb, and L. Szczecinski, "Spatial modulation: optimal detection and performance analysis," *IEEE Commun. Lett.*, vol. 12, no. 8, pp. 545–547, 2008.
- [62] R. Mesleh, S. Engelken, S. Sinanovic, and H. Haas, "Analytical SER calculation of spatial modulation," in *IEEE 10th International Symposium on Spread Spectrum Techniques and Applications*, Bologna, Italy, 25–28, August 2008, pp. 272–276.
- [63] R. Mesleh, S. Ganesan, and H. Haas, "Impact of channel imperfections on spatial modulation OFDM," in *IEEE 18th International Symposium on Personal, Indoor and Mobile Radio Communications*, Athens, Greece, 3–6 September 2007, pp. 1–5.
- [64] J. Jeganathan, A. Ghayeb, L. Szczecinski, and A. Ceron, "Space shift keying modulation for MIMO channels," *IEEE Trans. Wireless Commun.*, vol. 8, no. 7, pp. 3692–3703, 2009.
- [65] R. Mesleh, I. Stefan, H. Haas, and P. M. Grant, "On the performance of trellis coded spatial modulation," in *International ITG Workshop on Smart Antennas*, Berlin, Germany, 16–18 February 2009, pp. 1–8.
- [66] N. Serafimovski, M. Di Renzo, S. Sinanovic, R. Mesleh, and H. Haas, "Fractional bit encoded spatial modulation (FBE-SM)," *IEEE Commun. Lett.*, vol. 14, no. 5, pp. 429–431, 2010.
- [67] M. Di Renzo and H. Haas, "Space shift keying (SSK-) MIMO over correlated rician fading channels: Performance analysis and a new method for transmit-diversity," *IEEE Trans. Commun.*, vol. 59, no. 1, pp. 116–129, 2011.
- [68] J. da Silva and M. de Campos, "Spectrally efficient UWB pulse shaping with application in orthogonal PSM," *IEEE Trans. Commun.*, vol. 55, no. 2, pp. 313–322, 2007.
- [69] P. Zhang, I. Dey, S. Sugiura, and S. Chen, "Semi-blind adaptive space-time shift keying systems based on iterative channel estimation and data detection," in *IEEE 73rd Vehicular Technology Conference (VTC2011-Spring)*, Budapest, Hungary, 15–18 May 2011, pp. 1–5.
- [70] S. Sugiura, "Coherent versus non-coherent space-time shift keying for co-located and distributed MIMO systems," Ph.D. dissertation, School of Electronics and Computer Science, University of Southampton, Aug. 2010.
- [71] S. Sugiura, S. Chen, and L. Hanzo, "Generalized space-time shift keying designed for flexible diversity-, multiplexing- and complexity-tradeoffs," *IEEE Trans. Wireless Commun.*, vol. 10, no. 4, pp. 1–10, 2011, in press.
- [72] —, "A unified MIMO architecture subsuming space shift keying, OSTBC, BLAST and LDC," in *IEEE 72nd Vehicular Technology Conference (VTC2010-Fall)*, Ottawa, Canada, 6–9 September 2010, pp. 1–5.
- [73] J. Wang, X. Wang, and M. Madhian, "On the optimum design of space-time linear-dispersion codes," *IEEE Trans. Wireless Commun.*, vol. 4, no. 6, pp. 2928–2938, 2005.
- [74] C. Xu, S. Sugiura, S. X. Ng, and L. Hanzo, "Reduced-complexity noncoherently detected differential space-time shift keying," *IEEE Signal Process. Letters*, vol. 18, no. 3, pp. 153–156, 2011.
- [75] S. Chen, S. Sugiura, and L. Hanzo, "Semi-blind joint channel estimation and data detection for space-time shift keying systems," *IEEE Signal Process. Lett.*, vol. 17, no. 12, pp. 993–996, 2010.
- [76] A. Sendonaris, E. Erkip, and B. Aazhang, "Increasing uplink capacity via user cooperation diversity," in *IEEE International Symposium on Information Theory*, Cambridge, MA, 1998, p. 156.
- [77] J. N. Laneman and G. W. Wornell, "Energy-efficient antenna sharing and relaying for wireless networks," in *IEEE Wireless Communications and Networking Conference (WCNC)*, vol. 1, Chicago, IL, 2000, pp. 7–12.
- [78] M. Dohler, E. Lefranc, and H. Aghvami, "Space-time block codes for virtual antenna arrays," in *13th IEEE International Symposium on Personal, Indoor and Mobile Radio Communications (PIMRC)*, vol. 1, Lisbon, Portugal, 2002.
- [79] A. Sendonaris, E. Erkip, B. Aazhang, Q. Inc, and C. A. Campbell, "User cooperation diversity. Part I. System description," *IEEE Trans. Commun.*, vol. 51, no. 11, pp. 1927–1938, 2003.
- [80] —, "User cooperation diversity. Part II. Implementation aspects and performance analysis," *IEEE Trans. Commun.*, vol. 51, no. 11, pp. 1939–1948, 2003.
- [81] J. N. Laneman and G. W. Wornell, "Distributed space-time-coded protocols for exploiting cooperative diversity in wireless networks," *IEEE Trans. Inf. Theory*, vol. 49, no. 10, pp. 2415–2425, 2003.
- [82] B. Zhao and M. C. Valenti, "Distributed turbo coded diversity for relay channel," *Electronics letters*, vol. 39, p. 786, 2003.
- [83] J. N. Laneman and D. N. C. Tse and G. W. Wornell, "Cooperative diversity in wireless networks: Efficient protocols and outage behavior," *IEEE Trans. Inf. Theory*, vol. 50, no. 12, pp. 3062–3080, 2004.
- [84] M. Janani, A. Hedayat, T. E. Hunter, and A. Nosratinia, "Coded cooperation in wireless communications: space-time transmission and iterative decoding," *IEEE Trans. Signal Process.*, vol. 52, no. 2, pp. 362–371, 2004.
- [85] R. U. Nabar, H. Bolcskei, and F. W. Kneubuhler, "Fading relay channels: performance limits and space-time signal design," *IEEE J. Sel. Areas Commun.*, vol. 22, no. 6, pp. 1099–1109, 2004.
- [86] P. Tarasak, H. Minn, and V. K. Bhargava, "Differential modulation for two-user cooperative diversity systems," *IEEE J. Sel. Areas Commun.*, vol. 23, no. 9, pp. 1891–1900, 2005.
- [87] A. Bletsas, A. Khisti, D. P. Reed, and A. Lippman, "A simple cooperative diversity method based on network path selection," *IEEE J. Sel. Areas Commun.*, vol. 24, no. 3, pp. 659–672, 2006.
- [88] Y. Jing and B. Hassibi, "Distributed space-time coding in wireless relay networks," *IEEE Trans. Wireless Commun.*, vol. 5, no. 12, p. 3524, 2006.
- [89] Y. Li, B. Vucetic, T. F. Wong, and M. Dohler, "Distributed turbo coding with soft information relaying in multihop relay networks," *IEEE J. Sel. Areas Commun.*, vol. 24, no. 11, pp. 2040–2050, 2006.
- [90] L. Xiao, T. E. Fuja, J. Klierer, and J. Costello, "A network coding approach to cooperative diversity," *IEEE Trans. inf. theory*, vol. 53, no. 10, p. 3714, 2007.
- [91] A. Bletsas, H. Shin, and M. Z. Win, "Cooperative communications with outage-optimal opportunistic relaying," *IEEE Trans. Wireless Commun.*, vol. 6, no. 9, pp. 3450–3460, 2007.
- [92] Y. Jing and H. Jafarkhani, "Distributed differential space-time coding for wireless relay networks," *IEEE Trans. Commun.*, vol. 56, no. 7, pp. 1092–1100, 2008.
- [93] B. Sirkeci-Mergen and A. Scaglione, "Randomized space-time coding for distributed cooperative communication," *IEEE Trans. Signal Process.*, vol. 55, no. 10, pp. 5003–5017, 2007.
- [94] S. Sugiura, S. Chen, H. Haas, P. M. Grant, and L. Hanzo, "Coherent versus non-coherent decode-and-forward relaying aided distributed space-time shift keying," *IEEE Trans. Commun.*, vol. 59, 2011, in press.
- [95] S. Sugiura, S. Chen, and L. Hanzo, "Packet-reliability based decode-and-forward relaying aided distributed space-time shift keying," in *IEEE Global Communications Conference (GLOBECOM)*, Miami, Florida, USA, 6–10 December 2010.
- [96] M. Jiang and L. Hanzo, "Unitary linear dispersion code design and optimisation for MIMO communication systems," *IEEE Signal Process. Lett.*, vol. 17, no. 5, pp. 497–500, 2010.
- [97] O. Damen, A. Chkeif, and J. C. Belfiore, "Lattice code decoder for space-time codes," *IEEE Commun. Lett.*, vol. 4, no. 5, pp. 161–163, 2000.
- [98] L. Hanzo, L.-L. Yang, E.-L. Kuan, and K. Yen, *Single and Multi-carrier DS-CDMA: Multi-user Detection, Space-time Spreading, Synchronisation, Networking, and Standards*. John Wiley and IEEE Press, 2003.
- [99] Z. Yang, B. Lu, and X. Wang, "Bayesian Monte Carlo multiuser receiver for space-time coded multicarrier CDMA systems," *IEEE J. Sel. Areas Commun.*, vol. 19, no. 8, pp. 1625–1637, 2001.
- [100] R. Chen, J. S. Liu, and X. Wang, "Convergence analyses and comparisons of Markov chain Monte Carlo algorithms in digital communications," *IEEE Trans. Signal Process.*, vol. 50, no. 2, pp. 255–270, 2002.
- [101] A. Doucet and X. Wang, "Monte Carlo methods for signal processing: a review in the statistical signal processing context," *IEEE Signal Process. Mag.*, vol. 22, no. 6, pp. 152–170, 2005.
- [102] M. Dorigo and T. Stützle, *Ant Colony Optimization*. MIT Press, 2004.
- [103] K. K. Soo, Y. M. Siu, W. S. Chan, L. Yang, and R. S. Chen, "Particle-swarm-optimization-based multiuser detector for CDMA communications," *IEEE Trans. Veh. Technol.*, vol. 56, no. 5, pp. 3006–3013, 2007.



Shinya Sugiura (M'06) received the B.S. and M.S. degrees from Kyoto University, Kyoto, Japan, in 2002 and 2004, respectively, and the Ph.D. degree from University of Southampton, Southampton, UK, in 2010. Since 2004, he has been with Toyota Central R&D Laboratories, Inc., Japan. His research has covered a range of areas in communications, including space-time modulation/demodulation, turbo coding, cooperative communications, multiuser detection, automotive antenna design as well as vehicular ad hoc networking.

Dr. Sugiura has published over 35 research papers in various journals and conference proceedings. He was awarded IEEE AP-S Japan Chapter Young Engineer Award in December 2008.



Sheng Chen (M'90-SM'97-F'08) obtained a BEng degree from the East China Petroleum Institute, Dongying, China, in 1982, and a PhD degree from the City University, London, in 1986, both in control engineering. In 2005, he was awarded DSc from the University of Southampton, Southampton, UK. Since 1999 he has been with the School of Electronics and Computer Science, the University of Southampton, UK. He previously held research and academic appointments at the Universities of Sheffield, Edinburgh and Portsmouth, all in UK.

Professor Chen's recent research works include adaptive signal processing, wireless communications, modelling and identification of nonlinear systems, neural network and machine learning, finite-precision digital controller design, evolutionary computation methods, and optimization. He has published over 280 research papers. In the database of the world's most highly cited researchers in various disciplines, compiled by Institute for Scientific Information (ISI) of the USA, Prof. Chen is on the list of the highly cited researchers in the engineering category, see <http://www.ISIHighlyCited.com>.



Lajos Hanzo (M'91-SM'92-F'04) FEng, FIEEE, FIET, DSc received his degree in electronics in 1976 and his doctorate in 1983. During his 35-year career in telecommunications he has held various research and academic posts in Hungary, Germany and the UK. Since 1986 he has been with the School of Electronics and Computer Science, University of Southampton, UK, where he holds the chair in telecommunications. He has co-authored 20 John Wiley - IEEE Press books on mobile radio communications totalling in excess of 10 000 pages,

published about 1000 research papers and book chapters at IEEE Xplore, acted as TPC & General Chair of IEEE conferences, presented keynote lectures and been awarded a number of distinctions. Currently he is directing an academic research team, working on a range of research projects in the field of wireless multimedia communications sponsored by industry, the Engineering and Physical Sciences Research Council (EPSRC) UK, the European IST Programme and the Mobile Virtual Centre of Excellence (VCE), UK. He is an enthusiastic supporter of industrial and academic liaison and he offers a range of industrial courses. He is also an IEEE Distinguished Lecturer as well as a Governor of the IEEE VTS. Since 2007 he has been the Editor-in-Chief of the IEEE Press and since 2009 a Chaired Prof. also at Tsinghua University, Beijing. For further information on research in progress and associated publications please refer to <http://www-mobile.ecs.soton.ac.uk>